

*Original Article*

## Angiotensin II Type 1 Receptor Blocker Prevents Atrial Structural Remodeling in Rats with Hypertension Induced by Chronic Nitric Oxide Inhibition

Hidetoshi OKAZAKI<sup>1-3)</sup>, Tetsuo MINAMINO<sup>4)</sup>, Osamu TSUKAMOTO<sup>4)</sup>, Jiyoong KIM<sup>1)</sup>,  
Ken-ichiro OKADA<sup>4)</sup>, Masafumi MYOISHI<sup>1-3)</sup>, Masakatsu WAKENO<sup>1-3)</sup>,  
Seiji TAKASHIMA<sup>4)</sup>, Naoki MOCHIZUKI<sup>1,3)</sup>, and Masafumi KITAKAZE<sup>2)</sup>

The prevalence of atrial fibrillation (AF) increases in patients with hypertension. Angiotensin II is involved in structural atrial remodeling, which contributes to the onset and maintenance of AF in paced animal models. We investigated the role of angiotensin II in atrial structural remodeling in rats with hypertension. Ten-week-old male Wistar-Kyoto rats were randomly divided into 4 groups: a control group (no treatment), an *N*<sup>ω</sup>-nitro-L-arginine methyl ester (L-NAME) group (administered L-NAME, an inhibitor of nitric oxide synthase, 1 g/l in drinking water), an L-NAME+candesartan group (L-NAME plus candesartan—an angiotensin II receptor blocker (ARB)—at 0.1 mg/kg/day), and an L-NAME+hydralazine group (L-NAME plus hydralazine at 120 mg/l in drinking water). Eight weeks after treatment, the L-NAME group showed significantly higher systolic blood pressure than the control group (197±12 vs. 138±5 mmHg, *p*<0.05). Candesartan or hydralazine with L-NAME reduced systolic blood pressure to baseline. Chronic inhibition of NO synthesis increased the extent of fibrosis and transforming growth factor-β expression in atrial tissue, and both of these effects were prevented by candesartan, but not by hydralazine. Cardiac hypertrophy and dysfunction were induced in the L-NAME group, and these effects were also prevented by candesartan, but not by hydralazine. In contrast, the decrease in thrombomodulin expression in the atrial endocardium in hypertensive rats was restored by candesartan and hydralazine. The ARB prevented atrial structural remodeling, a possible contributing factor for the development of AF, in the hearts of rats with hypertension induced by long-term inhibition of NO synthesis. (*Hypertens Res* 2006; 29: 277–284)

**Key Words:** angiotensin II type 1 receptor blocker, atrial fibrillation, nitric oxide, hypertension, atrial remodeling

---

From the <sup>1)</sup>Department of Structural Analysis, National Cardiovascular Center Research Institute, Suita, Japan; <sup>2)</sup>Cardiovascular Division, National Cardiovascular Center, Suita, Japan; and <sup>3)</sup>Department of Bioregulatory Medicine and <sup>4)</sup>Department of Cardiovascular Medicine, Osaka University Graduate School of Medicine, Suita, Japan.

This study was supported by grants for research on Human Genome, Tissue Engineering, and Food Biotechnology (H13-Genome-11) and grants for Comprehensive Research on Aging and Health (H13-21seiki [seikatsu]-23) in Health and Labour Science Research from the Ministry of Health, Labour, and Welfare, Japan.

Address for Reprints: Tetsuo Minamino, M.D., Ph.D., Department of Cardiovascular Medicine, Osaka University Graduate School of Medicine, Suita 565-0871, Japan. E-mail: minamino@medone.med.osaka-u.ac.jp

Received September 7, 2005; Accepted in revised form January 13, 2006.

## Introduction

Atrial fibrillation (AF) is associated with a high risk of cardiovascular morbidity and mortality, and its prevalence is expected to double in the next 50 years (1–5). Patients with hypertension and chronic heart failure (CHF) are at high risk of developing AF (2, 6). The development and maintenance of AF are associated with changes in electrical and structural properties known as atrial remodeling (7, 8). Kumagai *et al.* demonstrated that rapid atrial pacing caused electrical and structural atrial remodeling (8). Li *et al.* demonstrated that CHF induced by rapid ventricular pacing strongly promotes the induction of sustained AF by causing fibrosis, which is a mechanism different from that of AF related to atrial tachycardia (7, 9). Importantly, both rapid atrial and ventricular pacing demonstrated that slowing of atrial conduction velocity is more important than shortening of the atrial effective refractory period in the development of AF, and that slowing of atrial conduction velocity is associated with extensive fibrosis (8, 9). Thus, the prevention of atrial fibrosis is a promising strategy for the management of AF. Although atrial structural remodeling, a possible contributing factor for the development and maintenance of AF, is observed in atrial and ventricular rapid pacing models (8, 9), it remains unknown whether it is involved in hypertensive hearts.

The renin-angiotensin system (RAS) is excessively activated in patients with CHF (10–13). Recent clinical data have clearly shown that the RAS suppression by treatment with an angiotensin-converting enzyme (ACE) inhibitor or an angiotensin type 1 receptor blocker (ARB) reduces the new onset of AF in patients with CHF (14–16). Consistent with the clinical data, RAS suppression by ACE inhibitors or ARBs prevents atrial structural remodeling in both rapid atrial and ventricular pacing models (8, 17). Recently, an ARB has been shown to confer better protection against the new onset of AF in hypertensive patients with left ventricular (LV) hypertrophy compared with a  $\beta$ -adrenergic receptor antagonist (18), suggesting that angiotensin II may also play an important role in the onset and maintenance of AF in hypertension. In the present study, we examined the occurrence of atrial structural remodeling and the role of angiotensin II in its development using candesartan, an ARB, in the hearts of rats with hypertension induced by long-term inhibition of nitric oxide (NO) synthesis (19). Furthermore, since atrial endocardial dysfunction such as a reduced thrombomodulin (TM) expression was previously induced in a rapid atrial pacing model (20, 21), we also investigated the effects of candesartan or hydralazine on TM expression in the atrium in this hypertensive model.

## Methods

### Materials

Candesartan was provided by Takeda Co., Ltd. (Osaka,

Japan), and the other drugs were obtained from Sigma Chemical Co. (St. Louis, USA). All procedures were performed in conformity with the Guide for the Care and Use of Laboratory Animals (NIH publication No. 93–23, revised 1985) and approved by the Osaka University Ethical Committee for Laboratory Animal Use.

### Animal Model of Chronic Inhibition of NO Synthesis

Since endothelial dysfunction has been documented in patients with CHF and hypertension (22, 23), which is largely the result of a decrease in the bioavailability of NO (24, 25), we adopted a hypertensive rat model induced by a long-term inhibition of NO synthesis. Ten-week-old male Wistar-Kyoto rats (Charles River, Yokohama, Japan) were randomly divided into 4 groups. The control group ( $n=11$ ) received no treatment. The  $N^{\omega}$ -nitro-L-arginine methyl ester (L-NAME) group ( $n=11$ ) received L-NAME at 1 g/l in drinking water. The L-NAME+candesartan group ( $n=11$ ) received L-NAME plus candesartan (0.1 mg/kg per day) orally. The L-NAME+hydralazine group received L-NAME plus hydralazine (120 mg/l in drinking water). Body weight (BW) was measured 1 week before and 8 weeks after the initiation of treatment. Blood pressure (BP) and heart rate (HR) were measured by the tail-cuff method 1 week before and 1, 2, 4, and 8 weeks after starting the experiments. All rats were housed, treated, and subjected to euthanasia as described previously (26).

### Echocardiographic Studies

Transthoracic echocardiography was performed using a machine equipped with a 7.5 MHz transducer (ALOKA Co., Ltd., Tokyo, Japan) after 8 weeks of treatment. Rats were anesthetized intraperitoneally with ketamine (15 mg/kg) and xylazine (5 mg/kg) and subjected to echocardiographic study. We measured echocardiographic parameters including LV end-diastolic dimension (LVDd), LV end-systolic dimension (LVDs), LV fractional shortening (LVFS), and the ratio of early to late filling wave of transmitral pulse-wave Doppler velocity ( $E/A$ ).

### Histopathological and Immunohistochemical Analysis

Eight weeks after treatment, rats in each group were sacrificed for morphometric, immunohistochemical and biochemical analyses. Excised hearts were weighed, separated into atrial and ventricular sections, cut, and stained with hematoxylin-eosin (HE) solution and Masson trichrome solution, and left atrial sections were carefully scanned as described previously (26). Each section was scanned at  $\times 200$  magnification. For immunohistochemistry, paraffin sections (5  $\mu$ m thick) were incubated overnight at 4°C with a rabbit polyclonal anti-

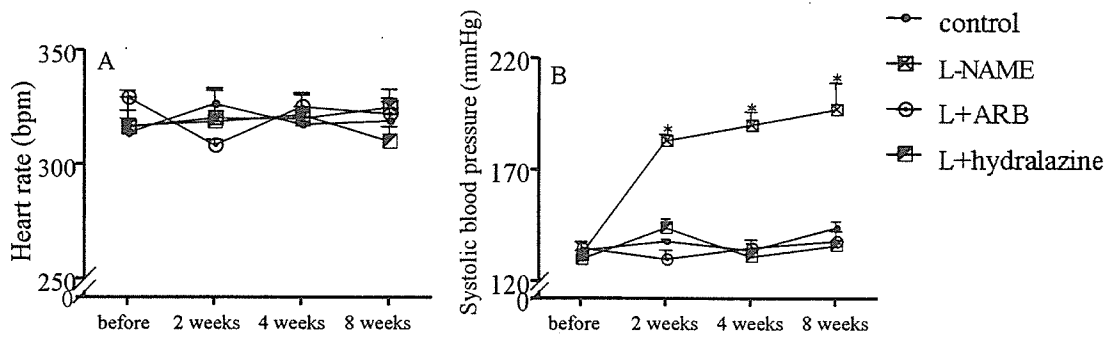


**Fig. 1.** Hemodynamic parameters in groups tested. A: Heart rate. B: Systolic blood pressure. L-NAME, N<sup>o</sup>-nitro-L-arginine methyl ester; L+ARB, N<sup>o</sup>-nitro-L-arginine methyl ester plus angiotensin II receptor blocker; L+hydralazine, N<sup>o</sup>-nitro-L-arginine methyl ester plus hydralazine. Data: mean  $\pm$  SEM. \* $p$  < 0.05 vs. control group.

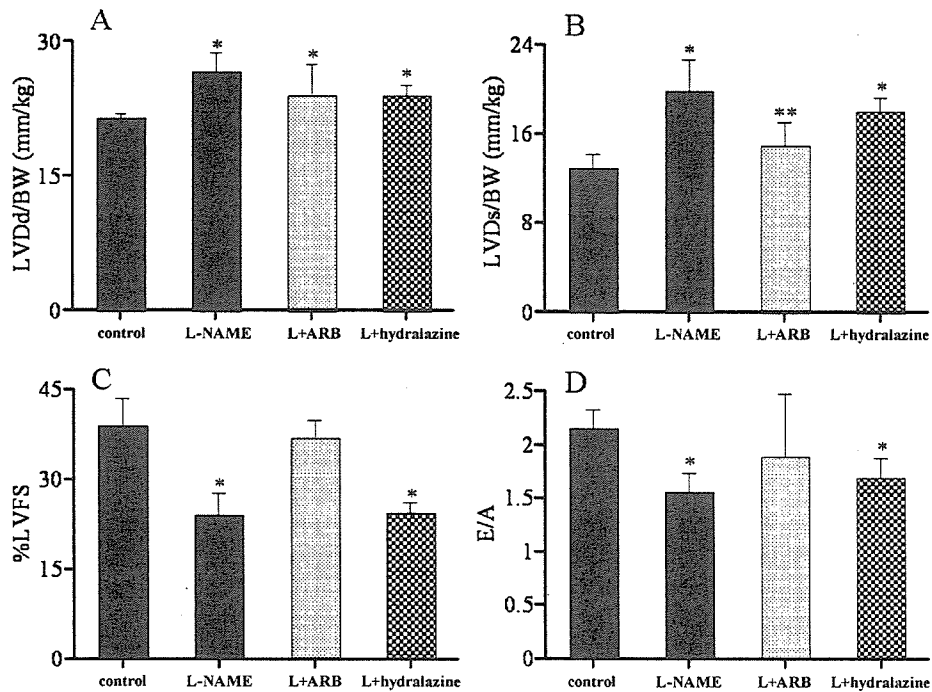


**Fig. 2.** Echocardiographic parameters in groups tested. A: Left ventricular end-diastolic dimension (LVDd) corrected by body weight (BW). B: Left ventricular end-systolic dimension (LVDs)/BW. C: Left ventricular fractional shortening (LVFS). D: E/A ratio (ratio of early to late filling wave velocity). L-NAME, N<sup>o</sup>-nitro-L-arginine methyl ester; L+ARB, N<sup>o</sup>-nitro-L-arginine methyl ester plus angiotensin II receptor blocker; L+hydralazine, N<sup>o</sup>-nitro-L-arginine methyl ester plus hydralazine. Data: mean  $\pm$  SEM. \* $p$  < 0.05 vs. control group, \*\* $p$  < 0.05 vs. L-NAME group.

TM antibody (American Diagnostica Inc., Stamford, USA). A goat polyclonal anti-rabbit IgG antibody (DAKO) was used as a secondary reagent.

#### Real-Time Quantitative Reverse Transcriptase-Polymerase Chain Reaction

Reverse transcriptase-polymerase chain reaction (RT-PCR) of left atrial samples of rat was performed according to the

Omniscript Reverse Transcription Handbook (QIAGEN Inc., Hilden, Germany). The rat primers and probes used for quantification of collagen type 1 and glyceraldehyde-3-phosphate-dehydrogenase (GAPDH) (internal control) were designed according to the manufacturer's protocol (Applied Biosystems, Foster City, USA) and those for transforming growth factor (TGF)- $\beta$  were designed as described previously (27). Real-time quantitative RT-PCR was performed with an ABI PRISM7700 Sequence Detection System (Applied Biosys-

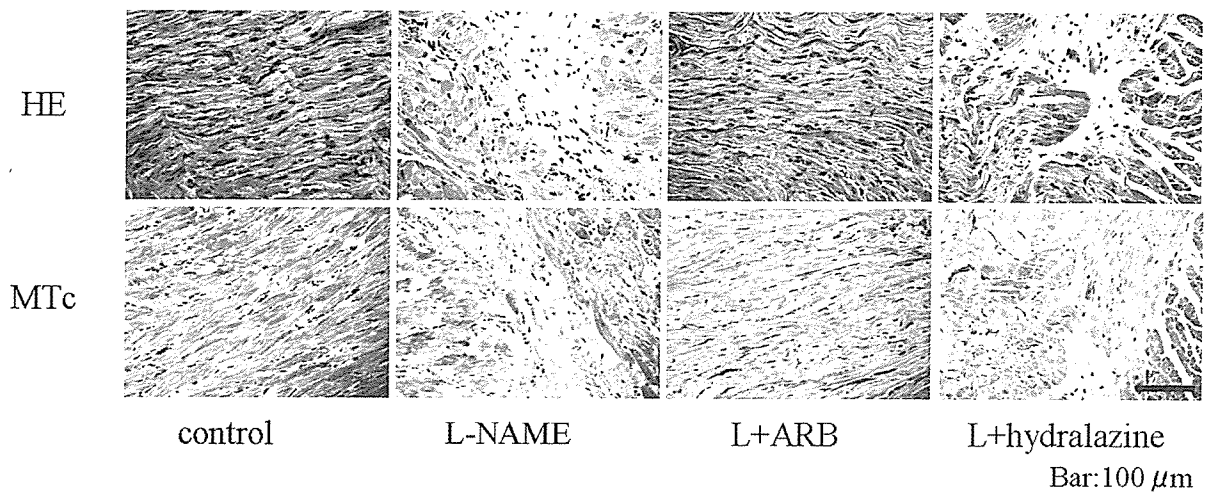


**Fig. 3.** Effects of angiotensin II receptor blocker (ARB) on atrial structural remodeling in the hypertensive rat model. Atrial sections were stained with hematoxylin-eosin (HE) and Masson's-Trichrome (MTc). The bar indicates 100 μm. L-NAME, N<sup>ω</sup>-nitro-L-arginine methyl ester; L+ARB, N<sup>ω</sup>-nitro-L-arginine methyl ester plus angiotensin II receptor blocker; L+hydralazine, N<sup>ω</sup>-nitro-L-arginine methyl ester plus hydralazine.

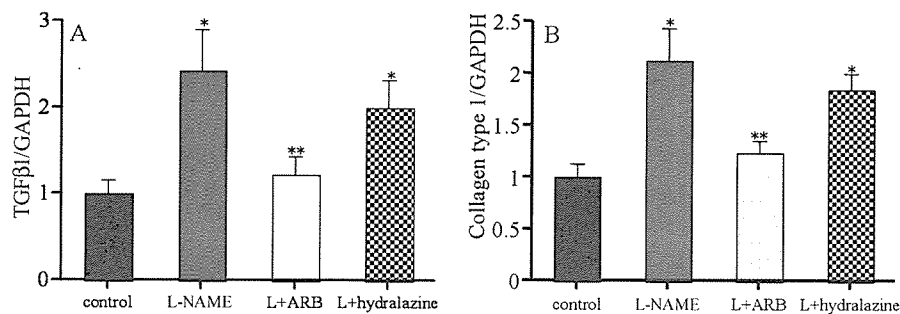


**Fig. 4.** Expression of collagen type 1 and transforming growth factor (TGF)-β in atrial tissue in the hypertensive rat model. Each sample of TGF-β 1(A) and collagen type 1(B) was normalized by glyceraldehyde-3-phosphate-dehydrogenase (GAPDH). L-NAME, N<sup>ω</sup>-nitro-L-arginine methyl ester; L+ARB, N<sup>ω</sup>-nitro-L-arginine methyl ester plus angiotensin II receptor blocker; L+hydralazine, N<sup>ω</sup>-nitro-L-arginine methyl ester plus hydralazine. Data: mean ± SEM. \*p < 0.05 vs. control group, \*\*p < 0.05 vs. L-NAME group.

tems) by the relative standard curve method. The target amount was determined from the relative standard curves constructed with serial dilutions of the control total RNA.

### Immunoblot Analysis

Protein extraction and immunoblot analysis of left atrial samples of rats were performed as described previously (20), and immunoreactive bands were quantified by densitometry (Molecular Dynamics, Sunnyvale, USA).

### Statistical Analysis

Data are expressed as the mean ± SEM. Heart weight (HW), BW, hemodynamic variables, collagen type 1 or TGF-β

expression normalized by GAPDH and TM protein levels were compared using one-way ANOVA followed by Bonferroni's test for multiple comparisons. Comparisons of the changes of BP among the groups over time were performed by two-way repeated-measures ANOVA followed by Bonferroni's correction, and values of p < 0.05 were considered to be statistically significant.

## Results

### Hemodynamic Parameters

HR and systolic BP (SBP) are presented in Fig. 1. The HR was comparable among the 4 groups tested and did not change throughout the study. SBP was comparable among the

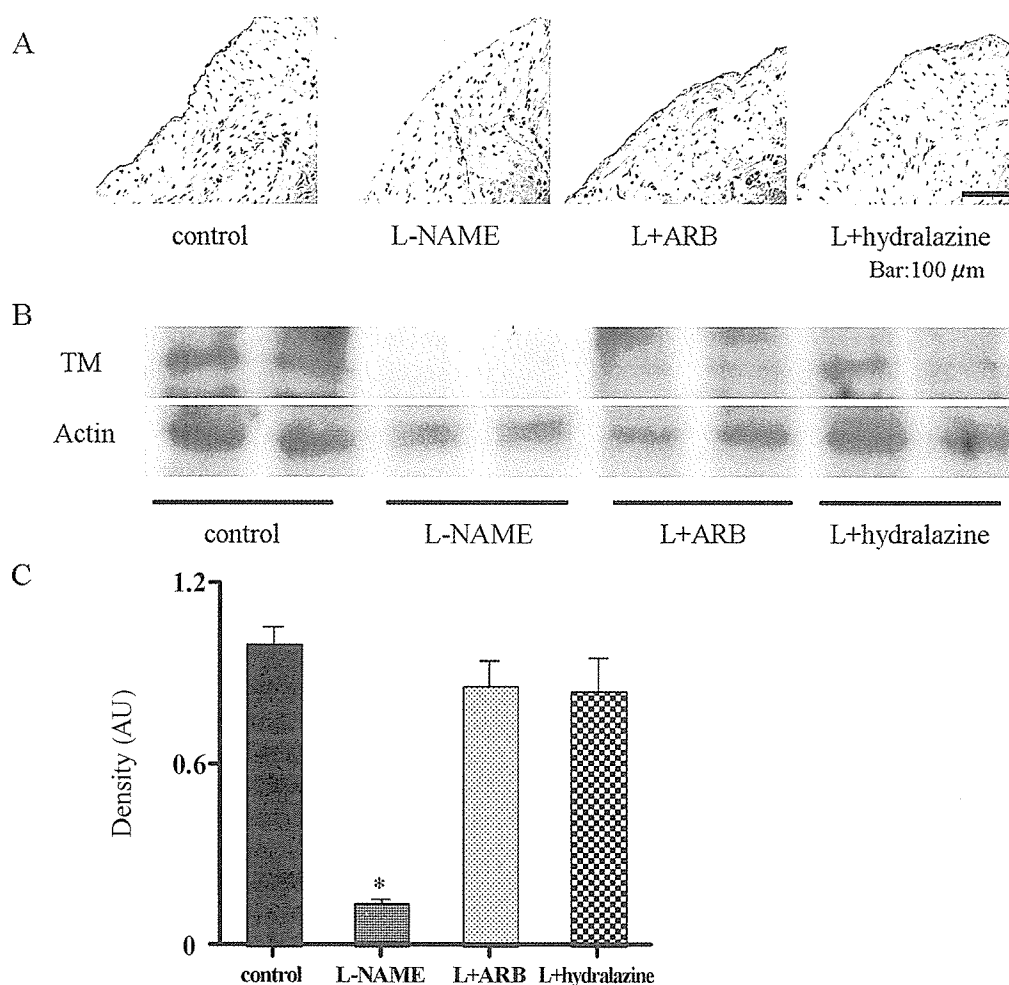


**Fig. 5.** Thrombomodulin (TM) expression in atrial tissues in the hypertensive rat model. *A:* Representative changes of TM expression in the atrial endocardium. The bar indicates 100 μm. *B:* Immunoblot analysis for TM protein expression in each group tested. *C:* Quantitative analysis of TM protein expression. L-NAME, N<sup>ω</sup>-nitro-L-arginine methyl ester; L+ARB, N<sup>ω</sup>-nitro-L-arginine methyl ester plus angiotensin II receptor blocker; L+hydralazine, N<sup>ω</sup>-nitro-L-arginine methyl ester plus hydralazine; AU, arbitrary unit. Data: mean ± SEM. \**p* < 0.05 vs. control group. N = 3.

4 groups before the study. In the L-NAME group, SBP increased progressively and became higher than that in the control group from 2 weeks of treatment onwards. The increase in SBP produced by L-NAME was decreased to the baseline by candesartan or hydralazine.

#### Effects of Candesartan and Hydralazine on Cardiac Hypertrophy and Dysfunction in Hypertensive Rats

The chronic treatment of rats with L-NAME significantly (*p* < 0.05) increased the HW/BW ratio compared with that in the controls (3.50 ± 0.05 vs. 2.89 ± 0.02). This increase was prevented by candesartan (2.98 ± 0.14), but not by hydralazine

(3.38 ± 0.07).

Quantitative echocardiographic data are presented in Fig. 2. Both LVDd/BW and LVDs/BW in the L-NAME group were significantly larger than in the control group. In the L-NAME group, LVFS was significantly decreased compared with that in the control group, indicating that systolic dysfunction was induced when NO synthesis was chronically inhibited. Candesartan, but not hydralazine, completely restored the reduction of LVFS by treatment with L-NAME. In addition, the *E/A* ratio in the L-NAME group was significantly decreased compared with that in the control group, indicating that diastolic dysfunction was also induced when NO synthesis was chronically inhibited. Candesartan, but not hydralazine, completely restored the reduction of *E/A* induced by L-NAME.

### Effects of Candesartan and Hydralazine on Atrial Structural Remodeling in Hypertensive Rats

The extent of atrial fibrosis in the L-NAME group 8 weeks after treatment was significantly greater than that in the control group. This fibrotic change was prevented by candesartan, but not by hydralazine (Fig. 3). Quantitative analysis by real-time RT-PCR demonstrated that the mRNA levels of collagen type I and TGF- $\beta$  in whole atrial tissue were significantly increased in the L-NAME group, while the increase in either molecule was reversed to the control levels by candesartan, but not by hydralazine (Fig. 4).

### Hemodynamic Effects on TM Expression in the Atrium of Hypertensive Rats

Eight weeks after treatment by L-NAME, immunohistological analysis revealed that TM expression on the atrial endocardial surface was markedly decreased (Fig. 5A). Treatment with candesartan or hydralazine comparably reversed the decrease in atrial TM levels induced by chronic inhibition of NO synthesis (Fig. 5B, C).

## Discussion

The present study demonstrated that candesartan, an ARB, but not hydralazine, prevented the progression of atrial fibrosis as well as LV hypertrophy and dysfunction in a hypertensive rat model induced by chronic inhibition of NO synthesis. Furthermore, candesartan and hydralazine comparably attenuated the reduction in TM expression in the atrial endocardium in this model. These findings suggest that angiotensin II plays an important role in the pathophysiology of atrial and ventricular structural remodeling in the hypertensive heart model. To our knowledge, the present study is the first to demonstrate a reduction of TM expression in left atrial tissue in hypertensive hearts.

Recent animal models of AF have proposed two principal forms of atrial remodeling: electrical remodeling, which affects cellular electrical properties, and structural remodeling, which alters the architecture of atrial tissue (7–9, 28). Atrial tachycardias cause ionic remodeling while decreasing the atrial refractory period and promoting atrial reentry (29, 30). By contrast, CHF produces extensive atrial interstitial fibrosis compared with atrial tachycardia, which promotes arrhythmogenesis by interfering with atrial conduction (7). Although Takemoto *et al.* clearly demonstrated that long-term inhibition of NO synthesis induces fibrotic changes in the left ventricle (31), the present study is the first to demonstrate structural atrial remodeling, a possible contributing factor for the development of AF, in the hypertensive heart model. Since we found extensive atrial fibrosis in this hypertension model, it is likely that the morphological changes in the atrium of hypertensive hearts are similar to those found in CHF rather than to those in atrial-tachycardia pacing. These

morphological differences in atrial tissue may reflect a difference in the pathophysiology of atrial fibrosis.

Recent clinical trials have demonstrated a reduction in the development and recurrence of AF by ACE inhibitors and ARBs in patients with CHF and hypertension (14, 32). Thus, the inhibition of the RAS is a novel concept for the prevention of AF that may target the underlying abnormalities of cardiac structure and electrical physiology that lead to AF. In the present study, candesartan, an ARB, but not hydralazine, prevented the progression of atrial fibrosis as well as LV hypertrophy and dysfunction in the hearts of hypertensive rats. There are two possible mechanisms by which candesartan prevented atrial structural remodeling in experimental hypertension with LV hypertrophy. One possible mechanism is the prevention of LV hypertrophy that may hemodynamically overload the atrium. LV hypertrophy is associated with a high incidence of AF in hypertensive patients (6). Thus, an anti-hypertensive drug, such as an ACE inhibitor or an ARB that can reverse LV hypertrophy, may effectively prevent the occurrence of AF (33). Indeed, in the LIFE study, an ARB, losartan, significantly reduced the incidence of AF compared with a  $\beta$ -adrenergic antagonist (18). The other possible mechanism is a direct anti-fibrotic effect of RAS inhibition. In both rapid atrial and ventricular pacing models, there are reports that the RAS inhibition by ACE inhibitors or ARB attenuates the development of atrial fibrosis that leads to the slowing of atrial conduction velocity (8, 9). Candesartan, an ARB, may reduce the extent of atrial fibrosis due to reduction of LV hypertrophy as well as its direct antifibrotic effect in hypertensive hearts. Furthermore, it is likely that an inverse agonist effect by candesartan will be beneficial for preventing activation of angiotensin II type I receptor due to atrial stretch (34).

Consistent with these atrial morphological changes, quantitative analysis by real-time RT-PCR demonstrated that mRNA levels of collagen and TGF- $\beta$  increased in this model. TGF- $\beta$  is a cytokine known to play an important role in stimulating fibrosis (35). In a transgenic mouse model, constitutional activation of TGF- $\beta$  produces atrial-restricted fibrosis and promotes inducibility of AF. Since angiotensin II induces the up-regulation of TGF- $\beta$  that leads to cardiac fibrosis (36), the attenuation of TGF- $\beta$  by the blockade of angiotensin II type I receptor may result in the reduction of fibrosis in atrial tissue.

Thrombin bound to endothelial TM cannot convert fibrinogen to fibrin or activate the anticoagulant protein C. Therefore, TM is considered to be a potent intrinsic anticoagulant factor (37), and the loss of TM in atria may lead to an increased risk of thromboembolism. In the hypertensive heart model induced by chronic inhibition of NO synthesis, we found that the expression of TM on the atrial endocardium was reduced. Interestingly, in contrast to the different effects of candesartan and hydralazine on atrial structural remodeling, candesartan and hydralazine comparably reduced systemic BP and restored the expression of TM. Thus, it is likely that atrial expression of TM is affected by hemodynamic fac-

tors such as systemic BP. However, we cannot deny the possibility that the local left atrial pressure may have been different, because the E/A ratios of the two groups were different. Since little is known about the modulators of TM expression, further investigation will be required into the mechanism by which the atrial expression of TM is regulated.

Patients with hypertension show endothelial dysfunction that may be largely attributable to reduced NO bioavailability (23–25). Thus, the hypertension model induced by long-term inhibition of NO synthesis will share the pathophysiology of patients with hypertension. We and other groups demonstrated that angiotensin II plays an important role in the development of LV fibrosis and cardiac inflammation in this model (25, 26, 38). However, the present study is the first to demonstrate the important role of angiotensin II in atrial remodeling in this hypertensive model. We must examine the role of angiotensin II in atrial structural remodeling in other hypertensive hearts.

A limitation of this study was that we did not demonstrate that atrial fibrosis in this hypertension model was associated with an increased vulnerability to AF or an increased incidence of AF. Future investigation will be required to check the relationship between atrial structural remodeling and the occurrence of AF in this hypertensive heart model.

In conclusion, atrial structural remodeling was observed in a hypertensive rat model. Blockade of angiotensin II type 1 receptor attenuated atrial fibrosis and the reduction in TM in the atrial endocardium. We need to consider pathophysiological atrial remodeling when we treat patients with hypertension.

### Acknowledgements

We thank Mr. Hirofumi Yukawa (ALOKA Co., Ltd.) for echocardiographic assistance, Ms. Yukari Arino for secretarial work, and Ms. Hiroko Okuda and Ms. Yoko Nagamachi for technical assistance.

### References

1. Benjamin EJ, Wolf PA, D'Agostino RB, Silbershatz H, Kannel WB, Levy D: Impact of atrial fibrillation on the risk of death: the Framingham Heart Study. *Circulation* 1998; **98**: 946–952.
2. Wang TJ, Larson MG, Levy D, et al: Temporal relations of atrial fibrillation and congestive heart failure and their joint influence on mortality: the Framingham Heart Study. *Circulation* 2003; **107**: 2920–2925.
3. Minamino T, Kitakaze M, Sanada S, et al: Increased expression of P-selectin on platelets is a risk factor for silent cerebral infarction in patients with atrial fibrillation: role of nitric oxide. *Circulation* 1998; **98**: 1721–1727.
4. Minamino T, Kitakaze M, Asanuma H, et al: Plasma adenosine levels and platelet activation in patients with atrial fibrillation. *Am J Cardiol* 1999; **83**: 194–198.
5. Minamino T, Kitakaze M, Sato H, et al: Plasma levels of nitrite/nitrate and platelet cGMP levels are decreased in patients with atrial fibrillation. *Arterioscler Thromb Vasc Biol* 1997; **17**: 3191–3195.
6. Verdecchia P, Reboldi G, Gattobigio R, et al: Atrial fibrillation in hypertension: predictors and outcome. *Hypertension* 2003; **41**: 218–223.
7. Li D, Fareh S, Leung TK, Nattel S: Promotion of atrial fibrillation by heart failure in dogs: atrial remodeling of a different sort. *Circulation* 1999; **100**: 87–95.
8. Kumagai K, Nakashima H, Urata H, Gondo N, Arakawa K, Saku K: Effects of angiotensin II type 1 receptor antagonist on electrical and structural remodeling in atrial fibrillation. *J Am Coll Cardiol* 2003; **41**: 2197–2204.
9. Shinagawa K, Li D, Leung TK, Nattel S: Consequences of atrial tachycardia-induced remodeling depend on the pre-existing atrial substrate. *Circulation* 2002; **105**: 251–257.
10. Cohn JN, Ferrari R, Sharpe N, on behalf of an International Forum on Cardiac Remodeling: Cardiac remodeling—concepts and clinical implications: a consensus paper from an international forum on cardiac remodeling. *J Am Coll Cardiol* 2000; **35**: 569–582.
11. Schnee JM, Hsueh WA: Angiotensin II, adhesion, and cardiac fibrosis. *Cardiovasc Res* 2000; **46**: 264–268.
12. Weber KT, Brilla CG: Pathological hypertrophy and cardiac interstitium. Fibrosis and renin-angiotensin-aldosterone system. *Circulation* 1991; **83**: 1849–1865.
13. Tanemoto M, Abe T, Obara N, Abe M, Satoh F, Ito S: Successful treatment of severe hypertension with the combination of angiotensin converting enzyme inhibitor and angiotensin II receptor blocker. *Hypertens Res* 2003; **26**: 863–868.
14. Vermees E, Tardif JC, Bourassa MG, et al: Enalapril decreases the incidence of atrial fibrillation in patients with left ventricular dysfunction: insight from the Studies of Left Ventricular Dysfunction (SOLVD) trials. *Circulation* 2003; **107**: 2926–2931.
15. Maggioni AP, Latini R, Carson PE, et al: Valsartan reduces the incidence of atrial fibrillation in patients with heart failure: results from the Valsartan Heart Failure Trial (Val-HeFT). *Am Heart J* 2005; **149**: 548–557.
16. Miura S, Saku K, Karnik SS: Molecular analysis of the structure and function of the angiotensin II type 1 receptor. *Hypertens Res* 2003; **26**: 937–943.
17. Shi Y, Li D, Tardif JC, Nattel S: Enalapril effects on atrial remodeling and atrial fibrillation in experimental congestive heart failure. *Cardiovasc Res* 2002; **54**: 456–461.
18. Wachtell K, Lehto M, Gerdtts E, et al: Angiotensin II receptor blockade reduces new-onset atrial fibrillation and subsequent stroke compared to atenolol: the Losartan Intervention for End Point Reduction in Hypertension (LIFE) study. *J Am Coll Cardiol* 2005; **45**: 712–719.
19. Egashira K, Ni W, Inoue S, et al: Pravastatin attenuates cardiovascular inflammatory and proliferative changes in a rat model of chronic inhibition of nitric oxide synthesis by its cholesterol-lowering independent actions. *Hypertens Res* 2000; **23**: 353–358.
20. Yamashita T, Sekiguchi A, Iwasaki YK, et al: Thrombomodulin and tissue factor pathway inhibitor in endocardium of rapidly paced rat atria. *Circulation* 2003; **108**: 2450–2452.
21. Li-Saw-Hee FL, Blann AD, Lip GY: A cross-sectional and

- diurnal study of thrombogenesis among patients with chronic atrial fibrillation. *J Am Coll Cardiol* 2000; **35**: 1926–1931.
22. Kubo SH, Rector TS, Bank AJ, Williams RE, Heifetz SM: Endothelium-dependent vasodilation is attenuated in patients with heart failure. *Circulation* 1991; **84**: 1589–1596.
  23. Panza JA, Quyyumi AA, Brush JE Jr, Epstein SE: Abnormal endothelium-dependent vascular relaxation in patients with essential hypertension. *N Engl J Med* 1990; **323**: 22–27.
  24. Node K, Kitakaze M, Yoshikawa H, Kosaka H, Hori M: Reduced plasma concentrations of nitrogen oxide in individuals with essential hypertension. *Hypertension* 1997; **30**: 405–408.
  25. Ribeiro MO, Antunes E, de Nucci G, Lovisolo SM, Zatz R: Chronic inhibition of nitric oxide synthesis. A new model of arterial hypertension. *Hypertension* 1992; **20**: 298–303.
  26. Minamino T, Kitakaze M, Papst PJ, *et al*: Inhibition of nitric oxide synthesis induces coronary vascular remodeling and cardiac hypertrophy associated with the activation of p70 S6 kinase in rats. *Cardiovasc Drugs Ther* 2000; **14**: 533–542.
  27. Kuwahara F, Kai H, Tokuda K, *et al*: Transforming growth factor-beta function blocking prevents myocardial fibrosis and diastolic dysfunction in pressure-overloaded rats. *Circulation* 2002; **106**: 130–135.
  28. Hoit BD: Matrix metalloproteinases and atrial structural remodeling. *J Am Coll Cardiol* 2003; **42**: 345–347.
  29. Yue L, Feng J, Gaspo R, Li GR, Wang Z, Nattel S: Ionic remodeling underlying action potential changes in a canine model of atrial fibrillation. *Circ Res* 1997; **81**: 512–525.
  30. Cha TJ, Ehrlich JR, Zhang L, Nattel S: Atrial ionic remodeling induced by atrial tachycardia in the presence of congestive heart failure. *Circulation* 2004; **110**: 1520–1526.
  31. Takemoto M, Egashira K, Usui M, *et al*: Important role of tissue angiotensin-converting enzyme activity in the pathogenesis of coronary vascular and myocardial structural changes induced by long-term blockade of nitric oxide synthesis in rats. *J Clin Invest* 1997; **99**: 278–287.
  32. Cohn JN, Tognoni G: A randomized trial of the angiotensin-receptor blocker valsartan in chronic heart failure. *N Engl J Med* 2001; **345**: 1667–1675.
  33. Dahlöf B, Herlitz H, Aurell M, Hansson L: Reversal of cardiovascular structural changes when treating essential hypertension. The importance of the renin-angiotensin-aldosterone system. *Am J Hypertens* 1992; **5**: 900–911.
  34. Zou Y, Akazawa H, Qin Y, *et al*: Mechanical stress activates angiotensin II type 1 receptor without the involvement of angiotensin II. *Nat Cell Biol* 2004; **6**: 499–506.
  35. Border WA, Noble NA: Transforming growth factor beta in tissue fibrosis. *N Engl J Med* 1994; **331**: 1286–1292.
  36. Kawano H, Do YS, Kawano Y, *et al*: Angiotensin II has multiple profibrotic effects in human cardiac fibroblasts. *Circulation* 2000; **101**: 1130–1137.
  37. Esmon CT: The roles of protein C and thrombomodulin in the regulation of blood coagulation. *J Biol Chem* 1989; **264**: 4743–4746.
  38. Takemoto M, Egashira K, Tomita H, *et al*: Chronic angiotensin-converting enzyme inhibition and angiotensin II type 1 receptor blockade: effects on cardiovascular remodeling in rats induced by the long-term blockade of nitric oxide synthesis. *Hypertension* 1997; **30**: 1621–1627.





ELSEVIER

Available online at [www.sciencedirect.com](http://www.sciencedirect.com)



Journal of Molecular and Cellular Cardiology 40 (2006) 666–674

Journal of  
Molecular and  
Cellular Cardiology

[www.elsevier.com/locate/yjmcc](http://www.elsevier.com/locate/yjmcc)

## Blockade of histamine H<sub>2</sub> receptors protects the heart against ischemia and reperfusion injury in dogs

Hiroshi Asanuma<sup>a</sup>, Tetsuo Minamino<sup>b</sup>, Akiko Ogai<sup>a</sup>, Jiyoong Kim<sup>a</sup>, Masanori Asakura<sup>a</sup>, Kazuo Komamura<sup>a</sup>, Shoji Sanada<sup>b</sup>, Masashi Fujita<sup>b</sup>, Akio Hirata<sup>b</sup>, Masakatsu Wakeno<sup>a</sup>, Osamu Tsukamoto<sup>a</sup>, Yoshiro Shinozaki<sup>c</sup>, Masafumi Myoishi<sup>a</sup>, Seiji Takashima<sup>b</sup>, Hitonobu Tomoike<sup>a</sup>, Masafumi Kitakaze<sup>a,\*</sup>

<sup>a</sup> Cardiovascular Division, National Cardiovascular Center, Suita, Suita City, Osaka Prefecture 565-8565, Tokai University School of Medicine, Isehara, Japan

<sup>b</sup> The Department of Internal Medicine and Therapeutics, Osaka University Graduate School of Medicine, Suita, Tokai University School of Medicine, Isehara, Japan

<sup>c</sup> Physiology Department, Tokai University School of Medicine, Isehara, Japan

Received 15 September 2005; received in revised form 3 February 2006; accepted 8 February 2006

Available online 17 April 2006

### Abstract

We have previously reported that histamine H<sub>2</sub> blockers may be cardioprotective in patients with chronic heart failure. Since both endogenous histamine and histamine H<sub>2</sub> receptors are present in heart tissue, we tested the hypothesis that the blockade of histamine H<sub>2</sub> receptors mediates protection against reversible or irreversible ischemia and reperfusion injury. In open-chest dogs, the left anterior descending coronary artery was occluded for 90 minutes, followed by reperfusion for 6 hours. Administration of famotidine and cimetidine from 10 minutes before occlusion until after 1 hour of reperfusion reduced infarct size (17.0 ± 4.1% and 17.8 ± 2.9% vs. 36.9 ± 5.9% of the solvent group, respectively). Famotidine administration only during the reperfusion period for 1 hour also attenuated infarct size (22.5 ± 3.5%). There were no differences in either area at risk or collateral flow among the groups. In another set of experiments, we decreased coronary perfusion pressure in dogs so that the coronary blood flow decreased to 50% of the non-ischemic level. In such conditions, we observed the increases in histamine release compared with non-ischemic conditions (0.04 ± 0.03 to 0.28 ± 0.13 ng/ml, *p* < 0.05). Famotidine improved anaerobic myocardial metabolism gauged by both lactate extraction ratio and myocardial oxygen consumption. We conclude that the blockade of histamine H<sub>2</sub> receptors mediates improvements in the anaerobic myocardial metabolism, and thus protects against ischemia and reperfusion injury.

© 2006 Elsevier Ltd. All rights reserved.

**Keywords:** Ischemia-reperfusion; Myocardial infarction; Coronary circulation; Histamine; Receptor pharmacology

### 1. Introduction

Histamine is one of the autacoids and provokes various cellular functions via the stimulation of four different G-protein-coupled receptors, i.e. histamine H<sub>1</sub>–H<sub>4</sub> receptors [1,2]. Histamine H<sub>2</sub> receptors, in particular, are known to be located in gastric cells and contribute to the production of acids that may cause gastric ulcers [1,3]. Therefore, the blockade of histamine H<sub>2</sub> receptors has been developed as a drug for the treat-

ment of gastric ulcers. Interestingly, we have previously reported that histamine H<sub>2</sub> blockers may be protective in patients with chronic heart failure (CHF) using the data mining technique [4], which enables us to find unexpected effective drugs for cardiovascular diseases [4]. In human ventricular tissue, histamine H<sub>1</sub> receptor expression was less abundant, whereas histamine H<sub>2</sub> receptors were highly expressed [5], and stimulation of H<sub>2</sub> receptors transduces the intracellular signals via the G<sub>s</sub> protein, as well as beta receptors [2,6]. Indeed, it is reported that:

1. histamine produces a positive inotropic effect in human ventricular muscles, likely due to the exclusive activation of H<sub>2</sub> receptors [7,8];

\* Corresponding author. Tel.: +81 6 6833 5012x2225;

fax: +81 6 6836 1120.

E-mail address: [kitakaze@zf6.so-net.ne.jp](mailto:kitakaze@zf6.so-net.ne.jp) (M. Kitakaze).

2. histamine exerts a positive chronotropic effect via the H<sub>2</sub> receptors [9];
3. and the blockade of histamine H<sub>2</sub> receptors decreases cardiac output in patients with CHF [10].

If these were the case, the blockade of histamine H<sub>2</sub> receptors protects the hearts against ischemia and reperfusion injury where histamine would be released in such a condition; beta-blockers are cardioprotective because catecholamine is released during ischemia and reperfusion.

We tested the hypothesis that the blockade of histamine H<sub>2</sub> receptors improves protection against ischemia and reperfusion injury in canine hearts. We also investigated whether histamine is released in response to ischemic stress and modulates the myocardial contractile and metabolic function in canine hearts with coronary hypoperfusion.

## 2. Materials and methods

### 2.1. Instrumentation

We have previously reported the details of the instrumentation procedure [11]. In brief, healthy adult beagle dogs for laboratory use (weighing 8–13 kg) were anesthetized with an intravenous injection of sodium pentobarbital (30 mg/kg), intubated, and ventilated using room air mixed with oxygen (100% O<sub>2</sub> at flow rate of 1.0–1.5 l/min). The arterial blood pH, pO<sub>2</sub>, and pCO<sub>2</sub> before starting the protocol were 7.37 ± 0.03, 103 ± 4 and 37.9 ± 1.9 mmHg, respectively. The chest was opened through the left fifth intercostals space, and the heart was suspended in a pericardial cradle. The proximal portion of the left anterior descending coronary artery (LAD) was cannulated and perfused with blood via the left carotid artery through an extracorporeal bypass tube. Coronary perfusion pressure (CPP) was monitored at the tip of the coronary arterial cannula, and coronary blood flow (CBF) in the perfused region was measured with an electromagnetic flow probe attached to the bypass tube. A small, short collecting tube (diameter 1 mm, length 70 mm) was inserted into a small coronary vein near the center of the perfused region to sample coronary venous blood. The drained venous blood was collected in a reservoir placed at the level of the left atrium and was returned via the jugular vein. Left ventricular pressure was measured with a micromanometer (Konigsberg P-5) placed through the apex into the left ventricular cavity. Two pairs of ultrasonic crystals were placed on the inner one third of the myocardium 1 cm apart to measure the myocardial segmental length with an ultrasonic dimension gauge (Schuessler, 5 MHz). End-diastolic length (EDL) was determined at the R wave on the electrocardiogram, and end-systolic length (ESL) was determined at the minimum pressure differential. Then, fractional shortening (FS) was calculated as [(EDL – ESL)/EDL] × 100%. Agents were administered into the LAD via the bypass tube. To constitute the coronary bypass between the carotid artery and the LAD, less than 30 s interruption of the LAD was necessary, but we confirm that this brief period of ischemia does not provoke either myocardial injury or protection. This study con-

formed to the “Position of the American Heart Association on Research Animal Use” adopted by the Association in November 1984.

## 3. Experimental protocols

### 3.1. Protocol I: Effects of the histamine H<sub>2</sub> blocker on myocardial metabolism and coronary blood flow in ischemic hearts

After the hemodynamics stabilization, coronary arterial and venous blood were sampled for blood gas analysis, and for the measurement of histamine [12], lactate [13] and the end-product (NO<sub>x</sub>) of nitric oxide (NO) levels [14,15]. The plasma histamine concentration was determined by the radioimmunoassay kit (SRL Co. Ltd.). Lactate extraction ratio (LER) was calculated as the coronary arterio-venous difference of the lactate concentration multiplied by 100 and divided by the arterial lactate concentration. Myocardial oxygen consumption (M $\dot{V}$ O<sub>2</sub>, ml/100 g per minute) was calculated as: CBF (ml/100 g per minute) × coronary arterial and venous blood oxygen difference (ml/dl).

To examine whether the administration of famotidine reduces the severity of myocardial ischemia, hemodynamic and metabolic parameters were monitored in 10 healthy adult beagle dogs. CPP was reduced so that CBF decreased to 50% of the baseline level for 5 min. After stabilization, either famotidine (16.7 μg/kg per min, an infusion rate of 0.0167 ml/kg per min at a concentration of 1.0 mg/ml, *N* = 5) or a solvent of famotidine (DMSO, 0.0167 ml/kg per minute, *N* = 5) was infused into the bypass tube for 20 min. After the measurements of hemodynamic parameters and blood samplings for the assessments of metabolic parameters, we quickly sampled endomyocardial tissue supplied by either LAD or left circumflex coronary artery (the non-ischemic area) into liquid nitrogen and stored it at –80 °C.

The famotidine was dissolved in DMSO before administration. A preliminary study showed that the dose of famotidine was the minimum dose required to cause maximum suppression of myocardial oxygen consumption without hemodynamic changes.

### 3.2. Methods for the measurements of plasma NO<sub>x</sub> levels, and myocardial cyclic AMP and Gs protein levels

The method for the measurement of NO<sub>x</sub> has been described previously [14,15]. Briefly, within 30 s of collection, heparinized blood was centrifuged for 5 min at 2000 × *g*. The plasma fraction was then diluted with an equal amount of nitrite/nitrate-free distilled water. Subsequently, 400 μl of diluted plasma was centrifuged at 200 × *g* through a micropore filter (Ultrafree MC Microcentrifuged Device, UFC3, Millipore, MA, USA) to remove substances larger than 10 kDa. The filtered plasma was analyzed using an automated procedure based on the Griess reaction. The amount of nitrite/nitrate within the sample was measured by its absorbance at 540 nm when mixed with the Griess reagent, 0.1% naphthylethlenediamide in 5%

H<sub>3</sub>PO<sub>4</sub>. The absorbance at 540 nm was also measured after passing the samples through a copper-plated cadmium column for nitrate reduction; this value expressed the total amount of plasma NO end-products (i.e. nitrate and nitrite). The cardiac NO level was defined as the differences in the level of the end-products of NO between coronary arterial and venous blood.

For the measurements of myocardial Gs protein levels, each frozen sample was homogenized mechanically in a homogenization buffer (20 mM Tris, 0.25 M sucrose, and 1 mM EDTA; pH 7.4), with a mechanical homogenizer. The homogenate was centrifuged at 600 × *g* for 5 minutes (4 °C) to remove nuclei and particulate cellular debris. A portion of the resulting supernatants was centrifuged at 250,000 × *g* for 1 hour to separate the membrane and cytosolic fractions. We measured Gs protein levels of the membrane fractions as previously reported [16] using a commercially available polyclonal antibody.

For the measurements of myocardial cyclic AMP (cAMP) levels, each sample of frozen muscle was homogenized mechanically in 500 ml of frozen hydrochloric acid (0.1 N) with a mechanical homogenizer. The homogenate was thawed and centrifuged at 5000 × *g* at room temperature for 15 minutes and the 100 ml aliquots of supernatant were subjected to the assay. Levels of cAMP were determined by a sensitive radioimmunoassay (cyclic AMP kit; Yamasa Shoyu Co., Choshi, Japan).

### 3.3. Protocol II: Effects of the histamine H<sub>2</sub> blockers on infarct size following 90 min of ischemia

In healthy adult beagle dogs, the bypass tube to the LAD was occluded for 90 min, followed by reperfusion for 6 hours, together with an intracoronary administration of famotidine (21.4 µg/kg per minute, an infusion rate of 0.0214 ml/kg per minute at a concentration of 1.0 mg/ml, famotidine group, *N* = 6), cimetidine (214 µg/kg per minute, an infusion rate of 0.0214 ml/kg per minute at a concentration of 10 mg/ml, cimetidine group, *N* = 6), promethazine (107 µg/kg per minute, an infusion rate of 0.0107 ml/kg per minute at a concentration of 5 mg/ml, promethazine group, *N* = 6) or the solvent (DMSO, 0.0214 ml/kg per minute, control group, *N* = 6) from 10 minutes before occlusion until after 1 hour of reperfusion. Promethazine is the selective antagonist of histamine H<sub>1</sub> receptors. Drugs were not infused during coronary occlusion. We also tested whether famotidine was effective when administered after the onset of reperfusion (famotidine after reperfusion). Famotidine (21.4 µg/kg per minute, an infusion rate of 0.0214 ml/kg per minute at a concentration of 1.0 mg/ml, *N* = 6) was infused into the bypass tube at the start of reperfusion for 1 hour of reperfusion (the famotidine (Rep) group). Hemodynamic parameters were monitored during myocardial ischemia and after the start of reperfusion. Infarct size was assessed 6 hours after the onset of reperfusion. A preliminary study showed that the doses of famotidine and cimetidine were the minimum doses required to cause the maximum infarct size-limiting effects without hemodynamic changes.

### 3.4. Measurements of infarct size and collateral blood flow

Six hours after the onset of reperfusion, while the LAD was reoccluded and perfused with autologous blood, Evans blue dye was injected into a systemic vein to identify the area at risk and the non-ischemic area in the hearts. The heart was then removed immediately, and sliced into serial transverse sections that were 6–7 mm in width. The non-ischemic area was defined as the tissue showing blue staining. The ischemic region was harvested and incubated at 37 °C for 20–30 minutes in 1% 2,3,5-triphenyltetrazolium chloride (TTC, Sigma Chemical Company) in 0.1 mol/l phosphate buffer adjusted to pH 7.4. TTC stains the non-infarcted myocardium a brick-red color, indicating the presence of a formazan product created through the reduction of TTC by dehydrogenases in viable tissues. In Protocol II, the area of myocardial necrosis and the area at risk were measured in all of the dogs on completion of the protocol by an operator who had no knowledge of the treatment given to each animal. Infarct size was expressed as a percentage of the area at risk.

Regional myocardial blood flow was determined as described previously [17]. Nonradioactive microspheres (Sekisui Plastic Co. Ltd., Tokyo, Japan) made of inert plastic were labeled with bromine (Br). The microspheres were administered 80 minutes after the start of coronary occlusion. The radio fluorescence of the stable heavy elements was measured with a wavelength dispersive spectrometer (PW 1480, Phillips Co. Ltd., Almelo, The Netherlands). Because the level of energy emitted is characteristic for specific elements, it was possible to quantify the radio fluorescence of the heavy element with which the microspheres were labeled. Myocardial blood flow was calculated according to the following formula: time flow = (tissue count) × (reference flow)/(reference count), and was expressed in milliliters per minute per gram wet weight. Endomyocardial blood flow was measured at the inner half of the LV wall.

### 3.5. Exclusion criteria

To ensure that all the animals used for analysis of infarct size in Protocol II were healthy and had been exposed to a similar extent of ischemia, the following standards were employed for the exclusion of unsatisfactory dogs: (1) subendocardial collateral blood flow greater than 15 ml/100 g per minute; (2) a heart rate greater than 170 beats/min; and (3) more than two consecutive attempts required to terminate ventricular fibrillation (VF) using low-energy DC pulses applied directly to the heart.

### 3.6. Statistical analysis

Statistical analysis was performed using ANOVA [18,19] to compare data among the groups. When ANOVA indicated a significant difference, paired data were compared using the Bonferroni test. Changes in the hemodynamic and metabolic parameters over time were assessed by ANOVA with repeated

Table 1  
Systemic hemodynamic parameters throughout the study (Protocol I)

Groups	Baseline	LF-5	D-5	D-10	D-20
<i>Mean blood pressure (mmHg)</i>					
1. Control group	102 ± 4	102 ± 4	102 ± 3	101 ± 3	101 ± 2
2. Famotidine group	99 ± 3	100 ± 2	99 ± 3	99 ± 3	98 ± 2
<i>Heart rate (min<sup>-1</sup>)</i>					
1. Control group	134 ± 5	134 ± 4	132 ± 4	131 ± 3	133 ± 4
2. Famotidine group	134 ± 4	134 ± 4	132 ± 4	131 ± 4	128 ± 4

Values are expressed as mean ± S.E.M. LF-5 = at 5 minutes of low flow, D-5, D-10 and 20 = at 5, 10 and 20 minutes after the onset of either famotidine or a solvent of famotidine (control) infusion, respectively. There were no significant changes of these parameters among the two groups. Statistical significance was tested by ANOVA.

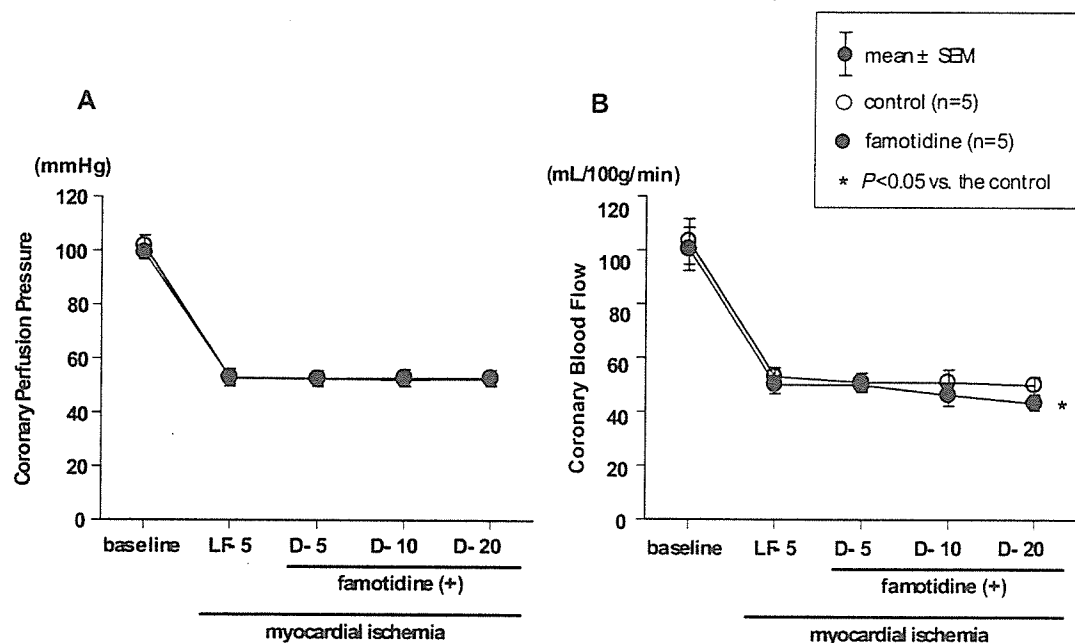


Fig. 1. Effects of famotidine on coronary hemodynamics in ischemic myocardium. A and B show the CPP and CBF, respectively. Abbreviations are the same as in Table 1. Data are mean ± S.E.M. \* $P < 0.05$  vs. the control (a solvent of famotidine) group. Statistical analysis was performed by ANOVA, followed by Bonferroni's test.

measures. Results were expressed as the mean ± S.E.M., with  $P < 0.05$  being considered significant.

#### 4. Results

##### 4.1. Effects of famotidine on myocardial anaerobic metabolism during coronary hypoperfusion

Before both CBF and CPP were reduced, there were no significant differences in the systemic hemodynamic and metabolic parameters (Table 1; Figs. 1 and 2). The reduction in both CPP and CBF increased the differences in histamine levels between coronary venous and arterial blood (dVA[histamine]) from  $0.04 \pm 0.03$  to  $0.28 \pm 0.13$  ng/ml ( $P < 0.05$ ,  $N = 5$ ), and cardiac NO levels prior to the administration of either famotidine or solvent in the famotidine and control groups (Fig. 3). The administration of a solvent did not affect CPP, FS, LER or  $M\dot{V}O_2$ . On the other hand, famotidine increased LER and decreased  $M\dot{V}O_2$  and CBF and a slight decrease in FS, even in the constant low-CPP state (Figs. 1 and 2), suggesting that

myocardial ischemia is improved by famotidine. The increment of cardiac NO levels was reduced by famotidine (Fig. 3).

Fig. 4 shows myocardial Gs protein levels and cAMP levels of the ischemic (the LAD artery-perfused area) and non-ischemic area (the left circumflex artery-perfused area) following 20 min of myocardial ischemia with and without an infusion of famotidine into the LAD. Although myocardial Gs protein levels were not modulated either by either famotidine or ischemia, the cAMP levels of the ischemic myocardium increased compared with those of the non-ischemic myocardium, and famotidine attenuated the ischemia-induced increases in myocardial cAMP levels.

##### 4.2. Effects of either famotidine or cimetidine on infarct size

Nine out of 45 dogs were excluded from analysis because their subendocardial collateral flow was greater than 15 ml/100 g per minute, so 36 dogs completed the protocol satisfactorily. Of these 36 dogs, nine developed VF at least once, with VF that matched the exclusion criteria occurring in six dogs, so these animals were also excluded from analysis. The number of

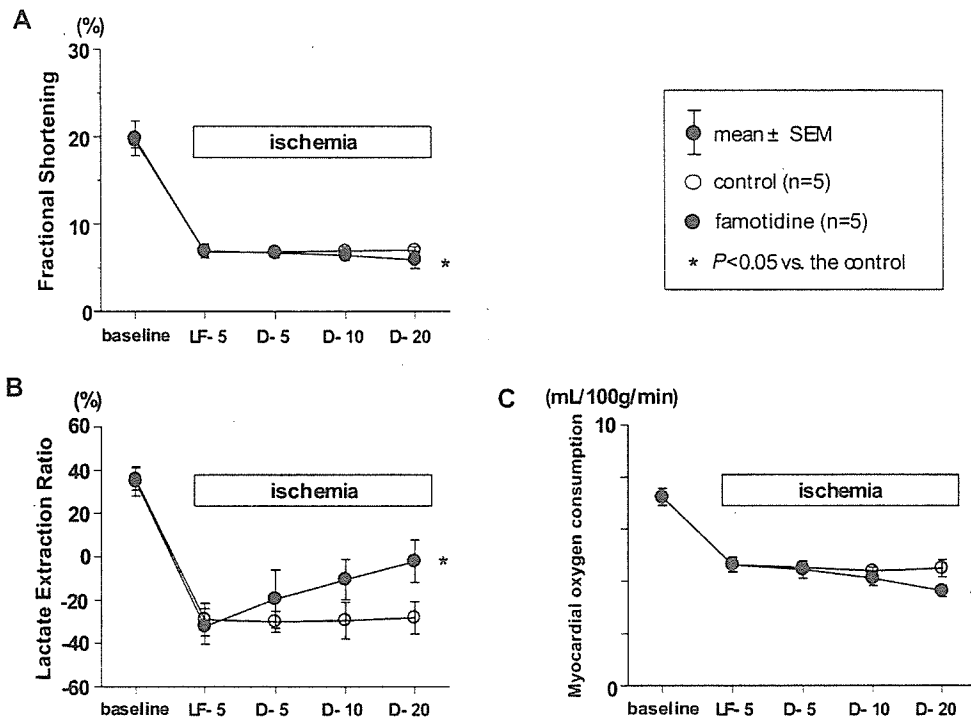


Fig. 2. Changes in fractional shortening (A), lactate extraction ratio (B) and myocardial oxygen consumption (C) in ischemic myocardium. Abbreviations are the same as in Table 1. Data are mean  $\pm$  S.E.M. \* $P < 0.05$  vs. the control (a solvent of famotidine) group. Statistical analysis was performed by ANOVA, followed by Bonferroni's test.

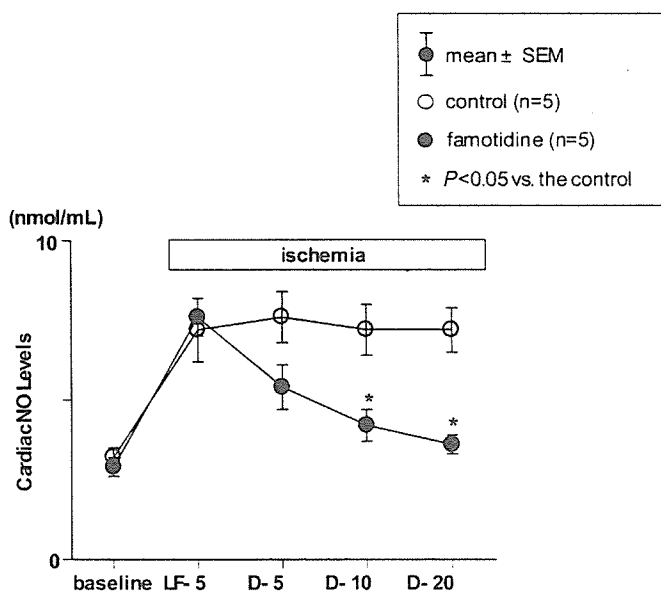


Fig. 3. Changes in cardiac NO levels during famotidine infusion in ischemic heart myocardium. Abbreviations are the same as in Table 1. Data are mean  $\pm$  S.E.M. \* $P < 0.05$  vs. the control (a solvent of famotidine) group. Statistical analysis was performed by ANOVA, followed by Bonferroni's test.

dogs that met the exclusion criteria of VF was 3, 1, 1, 1 and 0 in the control, famotidine, cimetidine, famotidine (Rep) or promethazine groups, respectively.

Neither aortic blood pressure nor heart rate showed any difference among the five groups throughout the protocol (Table 2). Table 3 shows the area at risk and the endocardial col-

lateral blood flow in the LAD region during myocardial ischemia. There were no significant differences in the area at risk and collateral flow among the five groups during myocardial ischemia. Fig. 5 shows that either famotidine or cimetidine decreased infarct size compared with the control groups. Furthermore, famotidine administration during an early reperfusion period also limited infarct size. However, a histamine  $H_1$  blocker, promethazine did not reduce infarct size.

## 5. Discussion

In the current study, we demonstrated that histamine release is increased from the ischemic myocardium, and the blockade of histamine  $H_2$  receptors improves anaerobic myocardial metabolism in ischemic hearts with reduced myocardial oxygen consumption. We also showed that the blockade of histamine  $H_2$  receptors limits infarct size but the blockade of histamine  $H_1$  receptors does not. These findings demonstrate that the blockade of histamine  $H_2$  receptors is beneficial against ischemia and reperfusion injury in canine hearts.

### 5.1. Histamine in ischemic hearts

We have shown that histamine release is augmented in the ischemic myocardium compared with the non-ischemic myocardium. Histamine is stored in mast cells, which, when stimulated, release histamine. There are reports that mast cells are found in the human heart [20], and have been implicated in cardiovascular diseases [21,22]. Indeed, an increase in mast cells has been observed in the hearts of hypertrophy [23], di-

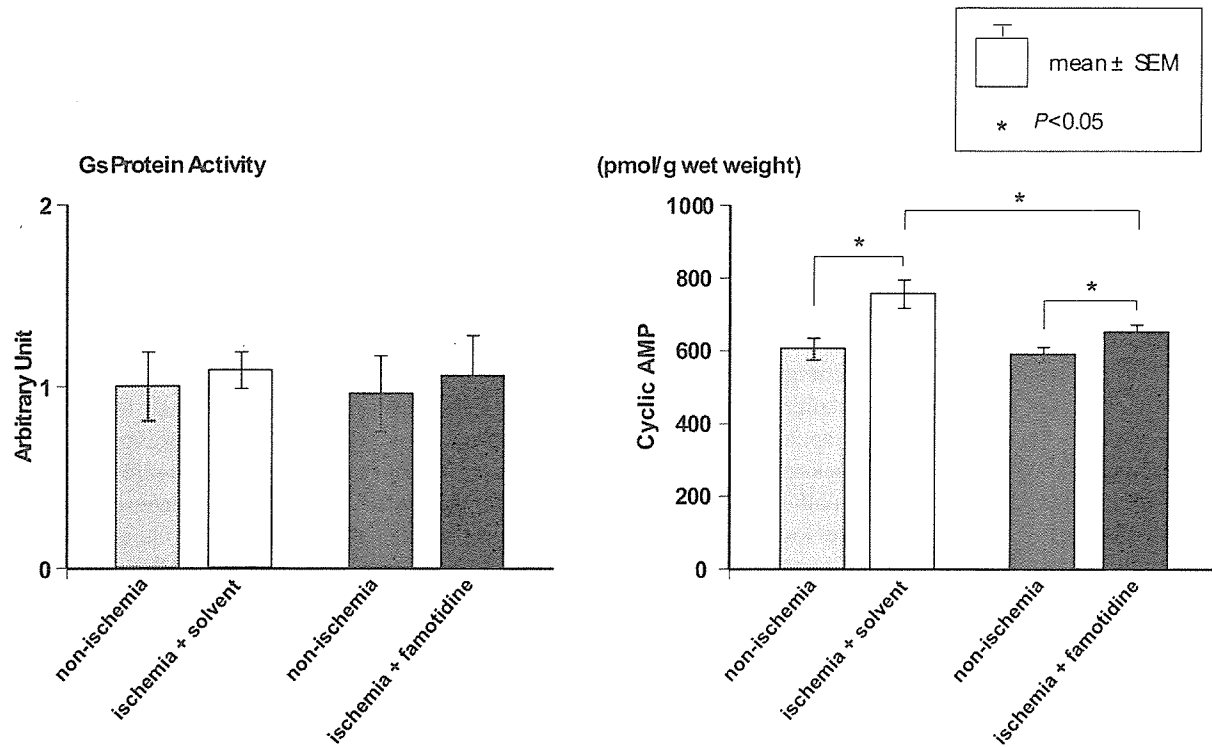


Fig. 4. Myocardial Gs protein levels and cAMP levels of the ischemic (the LAD artery-perfused area) and non-ischemic area (the left circumflex artery-perfused area) following 20 minutes of myocardial ischemia with and without famotidine.

Although myocardial Gs protein levels were not modulated by either famotidine or ischemia, the cAMP levels of the ischemic myocardium increase compared with those of the non-ischemic myocardium, and famotidine attenuated the ischemia-induced increases in myocardial cAMP levels. Statistical analysis was performed by ANOVA, followed by Bonferroni's test.

Table 2  
Systemic hemodynamic parameters throughout the study (Protocol II)

Groups	Baseline	D-10	Isc-90	Rep-60	Rep-180	Rep-360
<i>Mean blood pressure (mmHg)</i>						
1. Control group	97 ± 3	102 ± 5	97 ± 4	102 ± 5	102 ± 7	102 ± 7
2. Famotidine group	102 ± 4	98 ± 6	99 ± 6	98 ± 7	100 ± 7	97 ± 7
3. Cimetidine group	100 ± 2	99 ± 2	98 ± 2	102 ± 4	102 ± 5	96 ± 5
4. Famotidine after reperfusion group	102 ± 6	104 ± 6	100 ± 6	98 ± 4	98 ± 3	100 ± 4
5. Promethazine group	99 ± 4	101 ± 4	98 ± 5	99 ± 6	101 ± 6	98 ± 4
<i>Heart rate (min<sup>-1</sup>)</i>						
1. Control group	135 ± 5	135 ± 5	134 ± 4	131 ± 5	129 ± 6	128 ± 7
2. Famotidine group	135 ± 3	130 ± 2	131 ± 3	127 ± 2	126 ± 4	126 ± 3
3. Cimetidine group	134 ± 3	130 ± 4	129 ± 5	127 ± 8	125 ± 7	124 ± 4
4. Famotidine after reperfusion group	133 ± 5	131 ± 5	130 ± 4	128 ± 4	125 ± 5	125 ± 4
5. Promethazine group	132 ± 5	130 ± 5	131 ± 7	128 ± 6	128 ± 5	126 ± 6

Abbreviations are the same as in Table 1. Values are expressed as mean ± S.E.M. There were no significant changes of these parameters among the five groups. Statistical significance was tested by ANOVA.

Table 3  
The area at risk and collateral blood flow during myocardial ischemia in each group

Groups	Risk area (%)	Collateral blood flow during myocardial ischemia (ml/100 g per minute)
1. Control group	39.8 ± 1.7	8.4 ± 1.3
2. Famotidine group	40.8 ± 3.4	7.5 ± 1.6
3. Cimetidine group	39.7 ± 2.1	7.9 ± 1.7
4. Famotidine after reperfusion group	40.5 ± 1.8	8.0 ± 1.6
5. Promethazine group	37.3 ± 2.8	7.5 ± 2.0

Values are expressed as mean ± S.E.M. There were no differences of the area at risk and collateral blood flow among all of the groups. Statistical significance was tested by ANOVA.

lated cardiomyopathy, ischemic cardiomyopathy [24], and ischemia–reperfusion [25], and infarction-related coronary arteries [26]. Furthermore, histamine is present in high concentrations in cardiac tissues in most animal species, including humans [6,27,28], and its release from cardiac stores and subsequent actions on the heart may be of importance in the pathophysiology of heart disease, which agrees with the current observation of enhanced histamine release from the ischemic myocardium. We did not clarify whether histamine is released from mast cells or histaminergic neurons in the hearts or the mechanisms by which mast cells or histaminergic neurons are stimulated; however, we showed that histamine release detected in the coronary vein is increased in response to ischemic stress. Furthermore, we showed that the blockade of histamine receptors in the heart has an impact on the pathophysiology of ischemic heart diseases. These lines of previous and current evidence strongly support the importance of histamine in ischemia and reperfusion injuries in hearts.

### 5.2. The role of histamine receptors in ischemic hearts

The currently known histamine receptors ( $H_1$ ,  $H_2$ ,  $H_3$ , and  $H_4$ ) are all G protein-coupled molecules that transduce extracellular signals via Gq, Gs, and Gi/o, respectively [1,2,29]. Histamine  $H_2$  receptors, in particular, are linked to Gs proteins that facilitate the production of cAMP, as do  $\beta$ -adrenoceptors [30]. Histamine  $H_2$  receptor-stimulated cAMP accumulation or adenylyl cyclase activity has been demonstrated in a variety of tissues, including gastric cells [6,31], vascular smooth muscle cells [32], the brain [6,33], and cardiac tissue [6,34]. Indeed, in the present study, we found that the blockade of histamine  $H_2$  receptors attenuates the ischemia-induced increases in myocardial cAMP accumulation.

$\beta$ -Adrenoceptor blockers are known to protect ischemic or failing hearts because the accumulation of cAMP following the activation of  $\beta$ -adrenoceptors enhances myocardial contractility and oxygen consumption, and enhancements of myocardial contractility and oxygen consumption deteriorate the cardiac function [35,36]. The importance of  $\beta$ -adrenoceptors or  $\beta$ -adrenoceptor blockers in the pathophysiology of diseased hearts is attributable to the presence of catecholamine and  $\beta$ -adrenoceptors in the heart. Therefore, since both histamine  $H_2$  receptors and histamine are located in ischemic hearts, it is very likely that blockers of histamine  $H_2$  receptors protect against ischemia and reperfusion injury, as do  $\beta$ -adrenoceptor blockers. Indeed, we have shown that the blockade of the histamine  $H_2$  receptors is beneficial in ischemia and reperfusion injuries. Therefore, the same scenario can be considered for cardioprotection attributable to the blockade of histamine  $H_2$  receptors.

Histamine has been reported to cause NO release through histamine  $H_2$  receptors in porcine endothelial cell [37]. Therefore, histamine  $H_2$  blockers may decrease cardiac NO levels and increase coronary vascular resistance. Indeed, we observed that histamine  $H_2$  blockers reduces cardiac NO levels. This may be attributable to the attenuation of histamine-induced NO production, however, may be due to the fact that histamine  $H_2$  blockers attenuate the severity of myocardial ischemia, be-

cause the increased severity of myocardial ischemia increases NO production. Intriguingly, despite famotidine-induced decreases in NO release, we found that histamine  $H_2$  blockers are cardioprotective against ischemia and reperfusion injury. This suggests that histamine is cardio-deleterious against ischemia and reperfusion injury via activation of Gs proteins even with enhancements of NO production, and the elimination of the effects of histamine  $H_2$  receptors are protective as a whole.

Levi and coworkers have shown the presence of  $H_3$  receptors in the heart and demonstrated that activation of  $H_3$  receptors can inhibit norepinephrine release from cardiac nerve endings and this inhibition is closely related to the suppression of reperfusion-induced arrhythmia including VF [38,39]. The treatment with  $H_2$  receptor blockers could result in an unhindered stimulation of  $H_3$  receptors because cardiac histamine levels were shown to increase under the ischemic conditions. Then, the possibility that the effectiveness of  $H_2$  receptor blockers on myocardial ischemia and reperfusion injury may be, at least in part, due to the activation of  $H_3$  receptors. The stimulation of  $H_1$  receptors with histamine is known to impair atrioventricular (AV) conduction [40,41]. This AV conduction slowing may contribute to the development of VF in myocardial ischemia and reperfusion injury. Thus, we tested whether  $H_1$  receptor blocker, promethazine, shows some beneficial effects on myocardial ischemia and reperfusion injury in our model. Promethazine decreased VF because there were no dog that met the exclusion criteria of VF, but did not decrease infarct size (Fig. 5). In addition, it has been reported that histamine is a powerful vasoconstrictor in atherosclerotic coronary

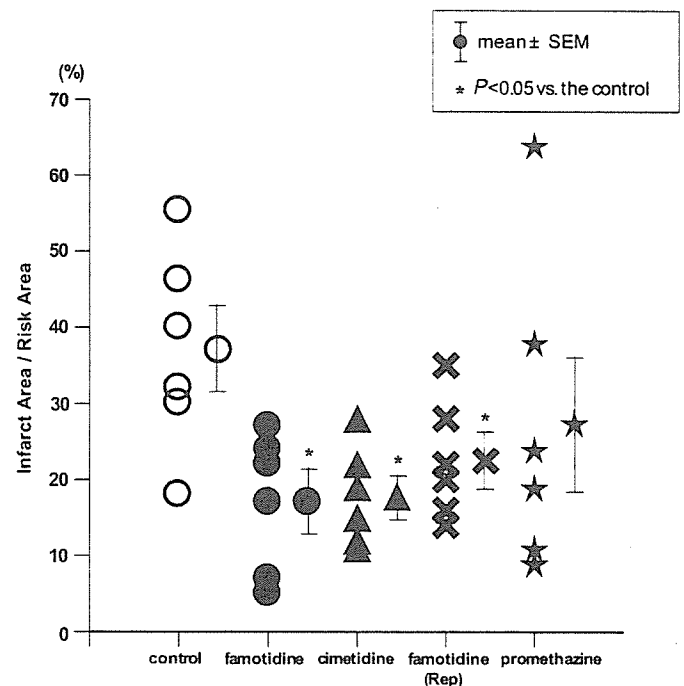


Fig. 5. Infarct size as a percentage of the area at risk. Infarct size was decreased in both the famotidine and cimetidine group compared with the control group. \*  $P < 0.05$  vs. the control (a solvent of famotidine) group. Statistical analysis was performed by ANOVA, followed by Bonferroni's test.

arteries [42], which may locally provoke coronary spasm and thus contribute to the onset of myocardial infarction [24].

### 5.3. Physiological and clinical relevance and the limitations of the present study

Since  $\beta$ -adrenoceptor blockers have been shown to be effective for the treatment of ischemic heart diseases and heart failure [43], and histamine receptor blockers are similar to  $\beta$ -adrenoceptor blockers, histamine plays an important role in the regulation and mal-regulation of cardiac and coronary functions. Furthermore, the histamine receptor blockers, such as famotidine and cimetidine, which are used to treat peptic ulcers all over the world, can be applied in ischemic heart diseases. Furthermore,  $\beta$ -adrenoceptor blockers ameliorate heart failure, especially ischemic heart failure, and the histamine receptor blockers may be beneficial for patients with CHF. This previous work hinted the present study. Therefore, we examined the effects of the histamine H<sub>2</sub> blocker on  $\dot{M}\dot{V}O_2$  and CBF in ischemic hearts in protocol I and the effects of the histamine H<sub>2</sub> blockers on infarct size following 90 min of ischemia in protocol II in the same condition, and found that the histamine H<sub>2</sub> blocker is cardioprotective against ischemia stress or reperfusion injury.

Fig. 2A and 2C show that both FS and  $\dot{M}\dot{V}O_2$  decreased after the administration of famotidine in ischemic conditions. However, it should be considered that the increases of both FS and  $\dot{M}\dot{V}O_2$  as index of the improvement of myocardial ischemia. The present results seem to be contradictory, but they are not. There are two strategies to reduce the ischemic burden of myocardium. One is to increase CBF, and another is to decrease myocardial workload. Ischemia per se decreases  $\dot{M}\dot{V}O_2$ . First of all, when CBF is increased,  $\dot{M}\dot{V}O_2$  and thus FS are increased along with the reduction of reversible or irreversible ischemic injury such as myocardial stunning or necrosis. Secondly, when myocardial workload is attenuated,  $\dot{M}\dot{V}O_2$  is further attenuated and FS is decreased along with the reduction of reversible or irreversible ischemic injury. Our previous work [11] that showed the increases in both CBF and  $\dot{M}\dot{V}O_2$  are attributable to the former mechanism for the attenuation of ischemic injury, and the present results that showed the decreased CBF and  $\dot{M}\dot{V}O_2$  are attributable to the latter mechanisms. In both cases, if the severity of ischemia decreases, LER, an index of anaerobic myocardial metabolism and severity of myocardial ischemia, is to be increased. The increases in LER were shown in the previous [11] and present studies, which show the improvements of myocardial ischemia via different mechanisms, i.e. the increased CBF- or decreased  $\dot{M}\dot{V}O_2$ -dependent mechanism.

On the other hand, Shen et al. [44] have shown that sodium pentobarbital severely inhibits myocardial mitochondrial function and greatly affects  $\dot{M}\dot{V}O_2$ . Thus, there may be some differences in myocardial energy metabolism including  $\dot{M}\dot{V}O_2$  and glucose, free fatty acid and lactate metabolism between awake and anesthetized conditions by pentobarbital.

Despite these limitations, if this hypothesis in the present work is validated further, histamine-related drugs or substances

may become candidates for the treatment of ischemic heart diseases or CHF.

Supported by grants-in-aid for scientific research from the Japanese Ministry of Education, Culture, Sports, Science and Technology (Nos.12470153 and 12877107); a Health and Labor Sciences Research Grant for Human Genome, Tissue Engineering and Food Biotechnology (H13-Genome-011); and a Health and Labor Sciences Research Grant for Comprehensive Research on Aging and Health (H13-21seiki(seikatsu)-23, H14Tokushitsu-38) from the Japanese Ministry of Health and Labor and Welfare.

### References

- [1] Leurs R, Bakker RA, Timmerman H, de Esch IJ. The histamine H<sub>3</sub> receptor: from gene cloning to H<sub>3</sub> receptor drugs. *Nat Rev Drug Discov* 2005;4:107–20.
- [2] Hough LB. Genomics meets histamine receptors: new subtypes, new receptors. *Mol Pharmacol* 2001;59:415–9.
- [3] Gantz I, Schaffer M, DelValle J, Logsdon C, Campbell V, Uhler M, et al. Molecular cloning of a gene encoding the histamine H<sub>2</sub> receptor. *Proc Natl Acad Sci USA* 1991;88:429–33.
- [4] Kim J, Washio T, Yamagishi M, Yasumura Y, Nakatani S, Hashimura K, et al. A novel data mining approach to the identification of effective drugs or combinations for targeted endpoints—application to chronic heart failure as a new form of evidence-based medicine. *Cardiovasc Drugs Ther* 2004;18:483–9.
- [5] Matsuda N, Jesmin S, Takahashi Y, Hatta E, Kobayashi M, Matsuyama K, et al. Histamine H<sub>1</sub> and H<sub>2</sub> receptor gene and protein levels are differentially expressed in the hearts of rodents and humans. *J Pharmacol Exp Ther* 2004;309:786–95.
- [6] Hill SJ, Ganellin CR, Timmerman H, Schwartz JC, Shankley NP, Young JM, Schunack W, Levi R, Haas HL. International Union of Pharmacology. XIII. Classification of histamine receptors. *Pharmacol Rev* 1997;49:253–78.
- [7] Eckel L, Gristwood RW, Nawrath H, Owen DA, Satter P. Inotropic and electrophysiological effects of histamine on human ventricular heart muscle. *J Physiol* 1982;330:111–23.
- [8] Du XY, Schoemaker RG, X462P6, Bos E, Saxena PR. Effects of histamine on porcine isolated myocardium: differentiation from effects on human tissue. *J Cardiovasc Pharmacol* 1993;22:468–73.
- [9] Hattori Y. Cardiac histamine receptors: their pharmacological consequences and signal transduction pathways. *Methods Find Exp Clin Pharmacol* 1999;21:123–31.
- [10] Kirch W, Halabi A, Hinrichsen H. Hemodynamic effects of quinidine and famotidine in patients with congestive heart failure. *Clin Pharmacol Ther* 1992;51:325–33.
- [11] Kitakaze M, Minamino T, Node K, et al. Beneficial effects of inhibition of angiotensin-converting enzyme on ischemic myocardium during coronary hypoperfusion in dogs. *Circulation* 1995;92:950–61.
- [12] Yamatodani A, Fukuda H, Wada H. High-performance liquid chromatographic determination of plasma and brain histamine without previous purification of biological samples: cation-exchange chromatography coupled with post-column derivatization fluorometry. *J Chromatogr* 1985;344:115–23.
- [13] Bergmeyer HU. In: *Methods of Enzymatic Analysis*. 1st ed. New York: NY: Academic Press Inc; 1963. p. 266–70 (1994; 93: 2197-205).
- [14] Green LC, Wagner DA, Glogowski J, et al. Analysis of nitrate, nitrite and [<sup>15</sup>N]nitrate in biological fluids. *Anal Biochem* 1982;126:131–8.
- [15] Node K, Kitakaze M, Kosaka H, et al. Plasma nitric oxide end products are increased in the ischemic canine heart. *Biochem Biophys Res Commun* 1995;211:370–4.
- [16] Hrbasova M, Novotny J, Hejnova L, Kolar F, Neckar J, Svoboda P. Altered myocardial Gs protein and adenylyl cyclase signaling in rats ex-



- posed to chronic hypoxia and normoxic recovery. *J Appl Physiol* 2003; 94:2423–32.
- [17] Mori H, Haruyama S, Shinozaki Y, Okino H, Iida A, Takanashi R, et al. New nonradioactive microspheres and more sensitive X-ray fluorescence to measure regional blood flow. *Am J Physiol* 1992;263:H1946–H1957.
- [18] Snedecor GW, Cochran WG. In: *Statistical Methods*. Iowa: Iowa State University Press; 1972. p. 258–98.
- [19] Steel RGD, Torrie JH. In: *Principles and Procedures of Statistics. A Biomedical Approach*. New York, NY: McGraw-Hill Publishing Co; 1980. p. 137–238.
- [20] Dvorak AM. Mast-cell degranulation in human hearts. *N Engl J Med* 1986;315:969–70.
- [21] Marone G, de Crescenzo G, Adt M, Patella V, Arbustini E, Genovese A. Immunological characterization and functional importance of human heart mast cells. *Immunopharmacology* 1995;31:1–18.
- [22] Hara M, Ono K, Hwang MW, Iwasaki A, Okada M, Nakatani K, et al. Evidence for a role of mast cells in the evolution to congestive heart failure. *J Exp Med* 2002;195:375–81.
- [23] Panizo A, Mindan FJ, Galindo MF, Cenarruzabeitia E, Hernandez M, Diez J. Are mast cells involved in hypertensive heart disease? *J Hypertens* 1995;13:1201–8.
- [24] Patella V, Marino I, Arbustini E, Lamparter-Schummert B, Verga L, Adt M, et al. Stem cell factor in mast cells and increased mast cell density in idiopathic and ischemic cardiomyopathy. *Circulation* 1998;97:971–8.
- [25] Frangogiannis NG, Perrard JL, Mendoza LH, Burns AR, Lindsey ML, Ballantyne CM, et al. Stem cell factor induction is associated with mast cell accumulation after canine myocardial ischemia and reperfusion. *Circulation* 1998;98:687–98.
- [26] Laine P, Kaartinen M, Penttila A, Panula P, Paavonen T, Kovanen PT. Association between myocardial infarction and the mast cells in the adventitia of the infarct-related coronary artery. *Circulation* 1999;99:361–9.
- [27] Wolff AA, Levi R. Histamine and cardiac arrhythmias. *Circ Res* 1986; 58:1–16.
- [28] Bristow MR, Ginsburg R, Harrison DC. Histamine and the human heart: the other receptor system. *Am J Cardiol* 1982;49:249–51.
- [29] Hofstra CL, Desai PJ, Thurmond RL, Fung-Leung WP. Histamine H4 receptor mediates chemotaxis and calcium mobilization of mast cells. *J Pharmacol Exp Ther* 2003;305:1212–21.
- [30] Lohse MJ, Engelhardt S, Eschenhagen T. What is the role of beta-adrenergic signaling in heart failure? *Circ Res* 2003;93:896–906.
- [31] Gespach C, Bouhours D, Bouhours JF, Rosselin G. Histamine interaction on surface recognition sites of H2-type in parietal and non-parietal cells isolated from the guinea pig stomach. *FEBS Lett* 1982;149:85–90.
- [32] Ottosson A, Jansen I, Edvinsson L. Pharmacological characterization of histamine receptors in the human temporal artery. *Br J Clin Pharmacol* 1989;27:139–45.
- [33] Al-Gadi M, Hill SJ. The role of calcium in the cyclic AMP response to histamine in rabbit cerebral cortical slices. *Br J Pharmacol* 1987;91:213–22.
- [34] Johnson CL, Weinstein H, Green JP. Studies on histamine H2 receptors coupled to cardiac adenylate cyclase. Blockade by H2 and H1 receptor antagonists. *Mol Pharmacol* 1979;16:417–28.
- [35] Packer M, Coats AJ, Fowler MB, Katus HA, Krum H, Mohacs P, et al. Effect of carvedilol on survival in severe chronic heart failure. *N Engl J Med* 2001;344:1651–8.
- [36] Dargie HJ. Effect of carvedilol on outcome after myocardial infarction in patients with left-ventricular dysfunction: the CAPRICORN randomised trial. *Lancet* 2001;357:1385–90.
- [37] Kishi F, Nakaya Y, Ito S. Histamine H2-receptor-mediated nitric oxide release from porcine endothelial cells. *J Cardiovasc Pharmacol* 1998;32: 177–82.
- [38] Imamura M, Poli E, Omoniyi AT, Levi R. Unmasking of activated histamine H3-receptors in myocardial ischemia: their role as regulators of exocytotic norepinephrine release. *J Pharmacol Exp Ther* 1994;271: 1259–66.
- [39] Hatta E, Yasuda K, Levi R. Activation of histamine H3 receptors inhibits carrier-mediated norepinephrine release in a human model of protracted myocardial ischemia. *J Pharmacol Exp Ther* 1997;283:494–500.
- [40] Levi R, Kuye JO. Pharmacological characterization of cardiac histamine receptors: sensitivity to H1-receptor antagonists. *Eur J Pharmacol* 1974; 27:330–8.
- [41] Hageman GR, Urthaler F, Isobe JH, James TN. Chronotropic and dromotropic effects of histamine on the canine heart. *Chest* 1979;75:597–604.
- [42] Ginsburg R, Bristow MR, Davis K, Dibiase A, Billingham ME. Quantitative pharmacologic responses of normal and atherosclerotic isolated human epicardial coronary arteries. *Circulation* 1984;69:430–40.
- [43] Metra M, Nardi M, Giubbini R, Dei Cas L. Effects of short- and long-term carvedilol administration on rest and exercise hemodynamic variables, exercise capacity and clinical conditions in patients with idiopathic dilated cardiomyopathy. *J Am Coll Cardiol* 1994;24:1678–87.
- [44] Shen W, Xu X, Ochoa M, Zhao G, Wolin MS, Hintze TH. Role of nitric oxide in the regulation of oxygen consumption in conscious dogs. *Circ Res* 1994;75:1086–95.

# Tricyclic pharmacophore-based molecules as novel integrin $\alpha_v\beta_3$ antagonists. Part IV: Preliminary control of $\alpha_v\beta_3$ selectivity by *meta*-oriented substitution

Dai Kubota, Minoru Ishikawa, Midori Ishikawa, Naokazu Yahata, Shoichi Murakami, Kazuyuki Fujishima, Masafumi Kitakaze<sup>†</sup> and Keiichi Ajito\*

Pharmaceutical Research Department, Meiji Seika Kaisha, Ltd, 760 Morooka-cho, Kohoku-ku, Yokohama 222-8567, Japan

Received 30 November 2005; revised 26 January 2006; accepted 27 January 2006

Available online 28 February 2006

**Abstract**—To establish the *in vivo* efficacy of  $\alpha_v\beta_3/\alpha_{IIb}\beta_3$  dual antagonists possessing a tricyclic pharmacophore, a corresponding  $\alpha_v\beta_3$ -selective antagonist was required as a control. We initially took two synthetic approaches to obtain  $\alpha_v\beta_3$ -selective antagonists based on the RGD recognition pattern or on modification of the dihedral angle between the central benzene ring and the adjacent heterocycle, but both proved unsuccessful. However, synthesis of novel antagonists with *meta*-substitution of the central benzene ring generated weak selectivity for  $\alpha_v\beta_3$  over  $\alpha_{IIb}\beta_3$  for the first time in the family of compounds with the tricyclic pharmacophore. Optimization of *meta*-oriented antagonists furnished an  $\alpha_v\beta_3$ -selective antagonist exhibiting inhibitory activity not only in a receptor-binding assay, but also in a cell adhesion assay.  
© 2006 Elsevier Ltd. All rights reserved.

## 1. Introduction

The vitronectin receptor, integrin  $\alpha_v\beta_3$ ,<sup>1,2</sup> is involved in the pathogenesis of various diseases in which cell adhesion or migration plays a key role. The function of integrin  $\alpha_v\beta_3$  in vascular smooth muscle cells and leukocytes led us to hypothesize that a potent  $\alpha_v\beta_3$  antagonist with an  $\alpha_{IIb}\beta_3$ -antagonistic effect, that is, a dual antagonist, would be a useful candidate for treatment of acute ischemic diseases, such as myocardial infarction or stroke.<sup>3</sup> In order to confirm the superior *in vivo* efficacy of dual antagonists possessing a tricyclic pharmacophore, we synthesized a corresponding  $\alpha_v\beta_3$ -selective antagonist as a control molecule. In our previous report,<sup>4</sup> we described the synthesis of the piperazine-based compound **1**, exhibiting strong  $\alpha_{IIb}\beta_3$  antagonism, and the piperidine-based compound **2**, showing  $\alpha_v\beta_3/\alpha_{IIb}\beta_3$  dual activity (Fig. 1). Here, we de-

scribe a successful approach to obtain selectivity for  $\alpha_v\beta_3$  over  $\alpha_{IIb}\beta_3$  in this class of compounds.

## 2. Synthetic approaches to $\alpha_v\beta_3$ -selective antagonists. Part I

Initially, we focused on the RGD recognition pattern to control selectivity. It is known that the simple existence

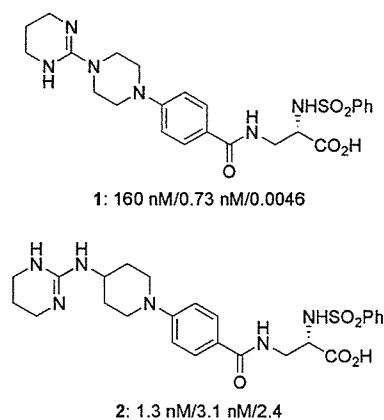


**Figure 1.** Reported integrin antagonists in our previous research. (IC<sub>50</sub>:  $\alpha_v\beta_3/\alpha_{IIb}\beta_3/\alpha_v\beta_3$  selectivity over  $\alpha_{IIb}\beta_3$ ).

**Keywords:** Integrin  $\alpha_v\beta_3$ -selective antagonist; Integrin  $\alpha_{IIb}\beta_3$  antagonist; Acute ischemic disease; *meta*-Oriented substitution.

\* Corresponding author at present address: R&D Strategy, R&D Planning and Management, Pharmaceutical, Meiji Seika Kaisha, Ltd, 2-4-16 Kyobashi Chuo-ku, Tokyo, 104-8002, Japan. Tel.: +81 3 3273 3346; fax: +81 3 3273 3380; e-mail: keiichi\_ajito@meiji.co.jp

<sup>†</sup> Director, Cardiovascular Division of Medicine, National Cardiovascular Center, 5-7-1 Fujishirodai, Suita, Osaka 565-8565, Japan.

of an RGD sequence is not necessarily sufficient for a molecule to serve as a ligand for  $\alpha_v\beta_3$ .<sup>5</sup> In fact, some molecules such as interstitial collagen type I have multiple RGD sequences for interaction with integrin  $\alpha_v\beta_3$ . Thus, we synthesized several dimeric molecules in an attempt to increase the interaction between integrin  $\alpha_v\beta_3$  and the candidate molecules, and thereby improve the  $\alpha_v\beta_3$  selectivity.

For construction of the dimers, two kinds of spacers were prepared (Scheme 1). The first dimer (**4**) with a C<sub>6</sub> spacer was directly synthesized using 2 equiv of compound **3**<sup>4</sup> with 1,6-dibromohexane in a low yield (less than 10%). The yield in the direct coupling of **3** with 1,12-dibromododecane, for synthesis of **5** with a longer spacer, was not improved. Then, a C<sub>12</sub> spacer was first introduced into the monomer (**3**) in a moderate yield to afford the alcohol **6**. Unfortunately, direct coupling of an alcohol **6** with the sulfonamide **3** according to a modified Mitsunobu protocol<sup>6</sup> did not give the desired dimer **5**. Thus, the alcohol was transformed to its iodide **7** via two steps, and **7** was successfully coupled with the sulfonamide **3** to furnish the dimer **5**. Dimers **4** and **5** were deprotected to afford the dimeric antagonists **8** and **9**, respectively. Compound **9** was further converted to a tetrahydropyrimidine analogue **10** by hydrogenolysis.

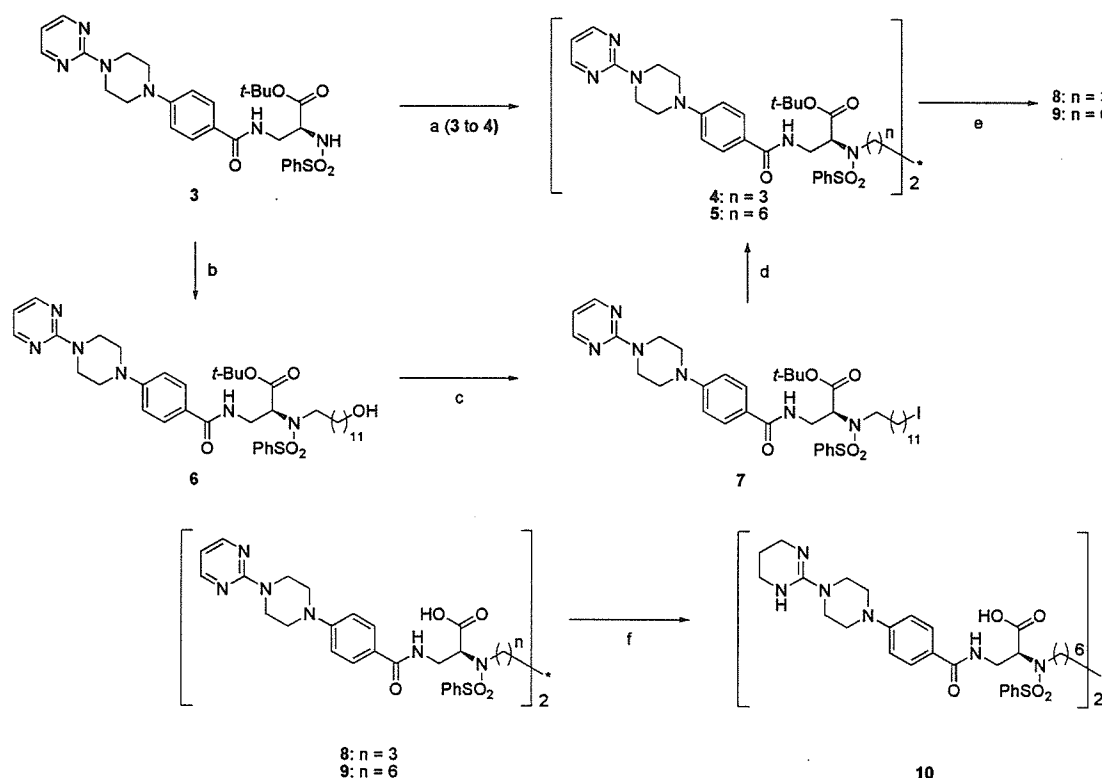
Although the  $\alpha_{IIb}\beta_3$ -antagonistic activity of some of these compounds was suppressed, none of them showed even weak  $\alpha_v\beta_3$  selectivity (Table 1).

### 3. Synthetic approaches to $\alpha_v\beta_3$ -selective antagonists. Part 2

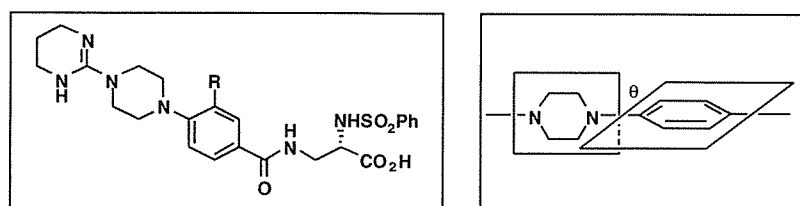
Our preliminary SAR data<sup>4</sup> showed that introduction of a halogen atom into the C-3 position at the central aromatic ring improved the  $\alpha_v\beta_3/\alpha_{IIb}\beta_3$ -antagonistic activity balance in tricyclic pharmacophore-containing compounds (Table 2). As a matter of fact, the calculated dihedral angle between the central benzene ring and the piperazine ring had a qualitative correlation only with  $\alpha_v\beta_3$ -antagonistic activity inhibition, not with  $\alpha_{IIb}\beta_3$ -antagonistic activity. Therefore, we planned to introduce a substituent onto the hetero ring to increase the dihedral angle. However, the 4-(2-methylpiperazin-1-yl)benzoate could not be synthesized by nucleophilic substitution, although the 4-(3-methylpiperazin-1-yl)benzoate could be prepared in a reasonable yield.

**Table 1.** Inhibitory activity of dimeric molecules in receptor-binding assay

Compound	Spacer ( <i>n</i> )	IC <sub>50</sub> (nM)		$\alpha_v\beta_3/\alpha_{IIb}\beta_3$
		$\alpha_v\beta_3$	$\alpha_{IIb}\beta_3$	
<b>1</b>	None	160	0.73	0.0046
<b>8</b>	6	70,000	43,000	0.61
<b>9</b>	12	29,000	3100	0.11
<b>10</b>	12	8800	11	0.0013



**Scheme 1.** Reagents and conditions: (a) 1,6-dibromohexane, DBU, DMF, rt, 12 days; (b) 12-bromododecanol, DBU, DMF, rt, 16 h; (c) i—MsCl, TEA, DMAP, CH<sub>2</sub>Cl<sub>2</sub>, rt, 16 h; ii—NaI, acetone, 40 °C, 40 h; (d) **3**, DBU, DMF, rt, 3 days; (e) TFA, anisole, CH<sub>2</sub>Cl<sub>2</sub>, 10 h, rt for **8**, 0–4 °C for **9**; (f) H<sub>2</sub>, Pd/C, AcOH, HCl, 3 atm, rt, 3 h.

**Table 2.** Effect of substitution of the central aromatic ring on inhibitory activity in receptor-binding assay

Compound	R	IC <sub>50</sub> (nM)		$\alpha_v\beta_3/\alpha_{IIb}\beta_3$	$\theta$ (deg)
		$\alpha_v\beta_3$	$\alpha_{IIb}\beta_3$		
1	H	160	0.73	0.0045	64.3
11	F	22	1.0	0.045	71.6
12	Cl	3.6	0.12	0.033	88.4

Modeling. All modeling experiments were done using the program package QUANTA/CHARMm (Accelrys Inc.) on SGI workstation.

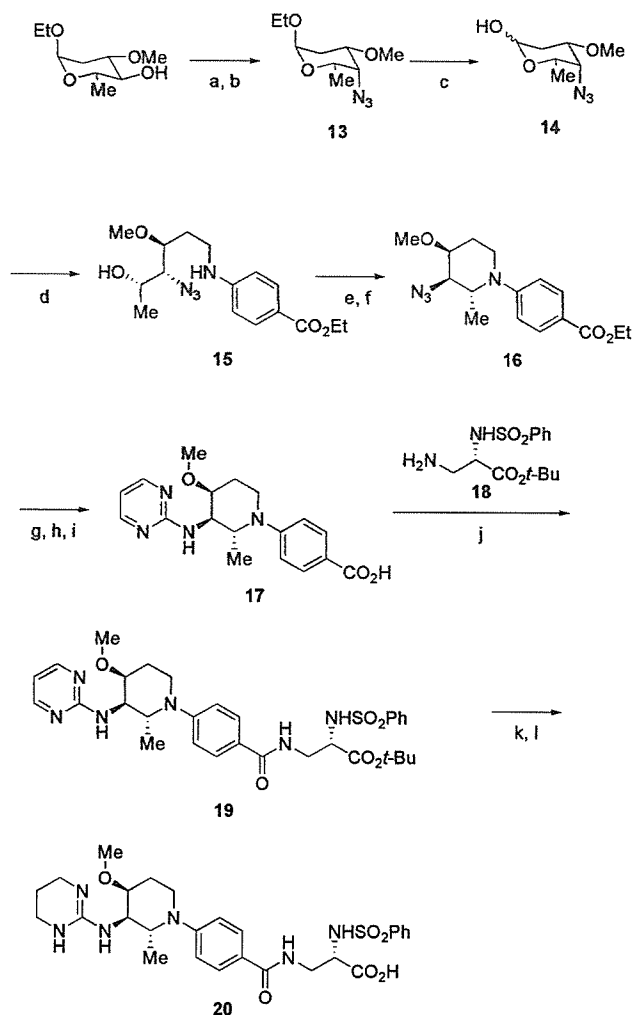
Then, we introduced a methyl group at the C-2 position of the hetero ring by utilizing a natural product (Scheme 2).

L-Oleandrose,<sup>7</sup> isolated as an  $\alpha$ -ethyl glycoside, was transformed to its azide derivative (13). After acidic hydrolysis, the obtained azide lactol 14 was reacted with ethyl 4-aminobenzoate by reductive amination to afford the key intermediate 15 with a linear substituent. Intramolecular cyclization of 15 proceeded via the mesylate to furnish a 2-methyl-heterocycle framework. Successive transformations gave the desired antagonist 20. Unfortunately, this molecule did not exhibit  $\alpha_v\beta_3$  selectivity ( $\alpha_v\beta_3$ : 7.8 nM,  $\alpha_{IIb}\beta_3$ : 3.4 nM, and  $\alpha_v\beta_3/\alpha_{IIb}\beta_3$ : 0.44).

#### 4. Synthesis of *meta*-oriented antagonists with $\alpha_v\beta_3$ selectivity

We next synthesized *meta*-oriented antagonists 21 and 22 as representative piperazine- and piperidine-based molecules, respectively (Fig. 2), based on the idea that the distance between the *N*-terminus and the *C*-terminus affects the selectivity for  $\alpha_v\beta_3$  over  $\alpha_{IIb}\beta_3$ .<sup>8</sup>

Nucleophilic substitution of 3-fluorobenzoate with a secondary amine-containing heterocycle did not proceed even under heating, in contrast to the reaction using 4-fluorobenzoate. However, nucleophilic substitution of 3-fluorobenzonitrile with 4-hydroxypiperidine was achieved to afford a *meta*-oriented intermediate, compound 23 (Scheme 3). The 4-hydroxypiperidine moiety was transformed to 4-aminopiperidine in three steps and reacted with 2-bromopyrimidine to construct the tricyclic pharmacophore. Acid hydrolysis of the benzonitrile moiety of 25 afforded the tricyclic benzoic acid (26). On the other hand, palladium-mediated coupling reaction<sup>9</sup> of 3-bromobenzoate with 4-hydroxypiperidine gave the *meta*-oriented benzoate 27 in a low yield. Sequential transformation of the piperidinone moiety, followed by introduction of pyrimidine, gave a tricyclic molecule (29), which was then converted to the intermediate 26 by basic hydrolysis. Moreover, the *meta*-oriented



**Scheme 2.** Reagents and conditions: (a) MsCl, Et<sub>3</sub>N, CH<sub>2</sub>Cl<sub>2</sub>, 0 °C, 2.0 h; (b) NaN<sub>3</sub>, DMF, 80 °C, 18 h; (c) HCl, 1,4-dioxane, 60 °C, 3.0 h; (d) NaBCNH<sub>3</sub>, ethyl 4-aminobenzoate, AcOH, CH<sub>2</sub>Cl<sub>2</sub>/MeOH, rt, 42 h; (e) MsCl, Et<sub>3</sub>N, CH<sub>2</sub>Cl<sub>2</sub>, 0 °C to rt, 2 h; (f) DIPEA, toluene, reflux, 18 h; (g) H<sub>2</sub>, Pd/C, rt, 18 h; (h) 2-bromopyrimidine, DIPEA, 120 °C, 18 h; (i) NaOH, MeOH/H<sub>2</sub>O, 50 °C, 6 h; (j) BOP, DIPEA, DMF, rt, 18 h; (k) TFA, CH<sub>2</sub>Cl<sub>2</sub>, rt, 3 h; (l) H<sub>2</sub>, Pd/C, 1,4-dioxane/H<sub>2</sub>O, rt, 18 h.